POLYAROMATIC CORES FOR ENHANCED CONDUCTIVITY IN INHERENTLY CONDUCTIVE POLYMERS

by

Xu Wang, M.E.

A thesis submitted to the Graduate Council of
Texas State University in partial fulfillment
of the requirements for the degree of
Master of Science with
a Major in Chemistry
August 2017

Committee Members:

Jennifer Irvin, Chair

Gary Beall

Alexander Kornienko

FAIR USE AND AUTHOR'S PERMISSION STATEMENT

Fair Use

Duplication Permission

DEDICATION

This thesis is dedicated to my fiancée, Yuan-fang Ying,
whose love encouraged me to pursue knowledge from a local town to Beijing,
and across the great Pacific Ocean to USA.

ACKNOWLEDGEMENTS

This work was supported by Partnership for Research and Education in Materials (PREM) NSF Grant DMR-1205670 and a Research Enhancement Grant from Texas State University.

The author would like to thank to Dr. Jennifer Irvin for her excellent comprehensive instruction on this thesis, as well as her psychological support during studying far from home. The guidance of other faculty at Texas State University has also been crucial to this thesis, especially the members of my committee, including Dr. Gary Beall and Dr. Alexander Kornienko. The author would like to thank to Dr. Ben Shoulders for his excellent training and instruction on NMR. The support from the lab members has played a significant role when encountering difficulties during research. The author would like the thank Alissa Kilian for her training on synthesis of graphene derivatives, Marisa Marquez for her electropolymerization of the monomer, and Dean Koehne for his training and discussion on conductivity measurement. Finally, the author would like to thank Dr. Mark Riggs for his instruction on graphene chemistry.

TABLE OF CONTENTS

Page

LIST OF TABLES

Table **Page**

LIST OF FIGURES

Figure **Page**

LIST OF ABBREVIATIONS

Abbreviation	Description
ICPs	Inherently Conductive Polymers
PPy	Polypyrrole
PANI	Polyaniline
PTh	Polythiophene
EDOT	3,4-ethylenedioxythiophene
PEDOT	Poly(3,4-ethylenedioxythiophene)
HWE	Horner-Wadsworth-Emmons
PEDOT: PSS	Poly(3,4-ethylenedioxythiophene) Polystyrene Sulfonate
PEDOT: Tos	Poly(3,4-ethylenedioxythiophene): Tosylate
GO	Graphene Oxide
HA	Humic Acid
FTIR	Fourier Transform Infrared Spectroscopy
NMR	Nuclear Magnetic Resonance
HSQC-NMR	Heteronuclear Single-Quantum Correlation Spectroscopy
COSY-NMR	Correlation Spectroscopy
TBAP	Tetrabutylammonium perchlorate
EtOAc	Ethyl Acetate
$CDCl_3$	Deuterated Chloroform
MeOH	Methanol

THF ..... Tetrahydrofuran

UV-Vis ..... Ultraviolet–Visible Spectroscopy

ABSTRACT

The discovery of Inherently Conductive Polymers (ICPs), also known as “synthetic metals”, is an attracting class of materials as a promising alternative for metallic semiconductors and conductors, which combine the positive properties of metals and conventional polymers with ease of synthesis and flexible processing techniques.

These polymers are useful for energy storage, electrochromics, corrosion protection, thermoelectric materials, chemical and biomedical sensors, and so on. Despite the excellent electrical conductivity along the length of each conjugated chain of ICPs, the electron hopping required for conduction from chain to chain results in series resistance.
The hypothesis of this thesis is that the electron hopping can be minimized by providing alternative conjugated pathways in the ICPs using a variety of polyaromatic cores.

Starting from a model compound, a tetrafunctionalized pyrene novel monomer was designed and synthesized using a pyrene core coupled with 3,4-ethylenedioxythiophene (EDOT) via vinylene linkages using the Horner-Wadsworth-Emmons (HWE) reaction. Characterizations confirmed the monomer, from which several polymers were prepared via both oxidative chemical polymerization and electropolymerization. The conductivity of the resulting polymers was investigated using four-point collinear probe.

The same technique can be applied to generate graphene-based hyperbranched ICPs. The functionalized graphene hub with aldehyde groups on the edges (graphenal) can be coupled with EDOT to yield a hyperfunctionalized monomer that can be polymerized to form a highly conjugated network with enhanced conductivity.

1. INTRODUCTION

1.1 The History of Inherently Conductive Polymers

Inherently Conductive Polymers (ICPs), also known as "synthetic metals", are an attracting class of materials that have been considered as a possible substitute for metallic semiconductors and conductors, which combine the positive properties of metals and conventional polymers, *i.e.*, great optical behavior and promising electrical conductivity, ease of synthesis, and flexibility in processing.[1,2]

The reversible redox behavior, involving changes in conductivity, color and volume by switching between two or more stable oxidation and reduction states,[3] and the unique combination of properties of metal and traditional polymers have led to applications in electrochromic, light-emitting diodes, actuators, corrosion inhibition, gas separation, sensors, energy storage, tissue engineering, and supercapacitors.[4] Since the last decades, several research groups have devoted to achieving those tailored ICPs with electrical, optical and thermal properties.

In 1977, the first ICP - doped polyacetylene - was produced by Shirakawa and coworkers;[5] since then more than 25 types of ICPs have been developed (Fig.1) Early researchers working on ICPs noticed that the conductivity of polyacetylene, whose conductivity was normally no better than semiconductor materials, was greatly improved by 10 million times when it was oxidized using iodine vapor.[5,6] This phenomenon triggered researchers into this novel area. The mechanism underlying the phenomenon is well known as "doping" that is essential to obtain the enhanced conductivity of ICPs.[1]

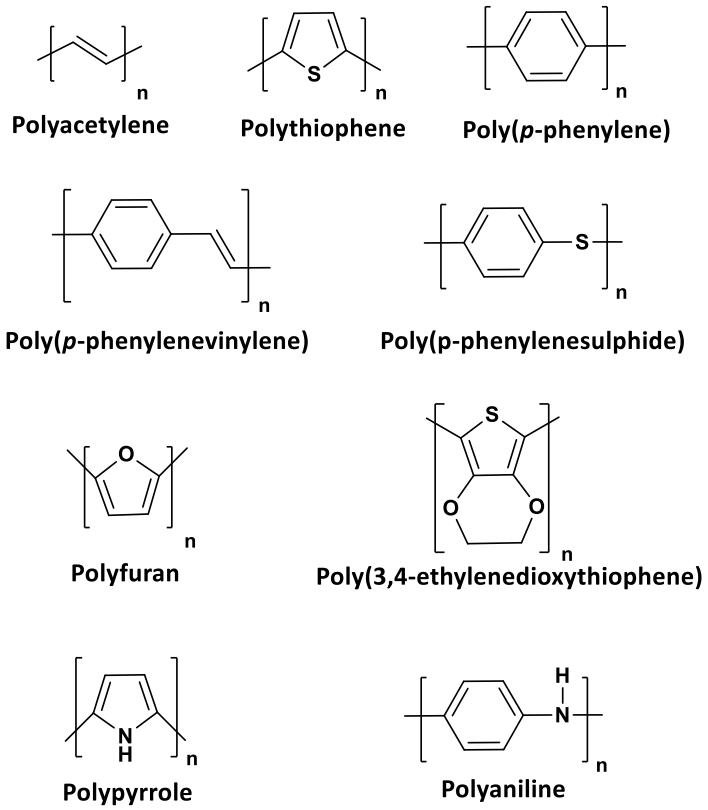

Figure 1. The repeat units of some representative ICPs

Due to its difficult synthesis and instability in air, polyacetylene is not a desirable candidate, which inspired researchers to search for more suitable ICPs.[6] Polyheterocycles since then have raised up as important members of ICPs family with a tailored combination of good stability and high conductivity,[7] and all the currently well-studied ICPs, *e.g.*, polypyrrole, polyaniline, and polythiophenes, belong to this domain.

1.1.1 Polypyrrole

Polypyrrole (PPy) and its derivatives have been intensively studied during the past decades due to their great electrical and optical properties.[8,9] Also, they are widely used as "smart" stimuli responsive biomaterials, allowing dynamic control of their properties.[10-12]

Different possible structures of PPy are demonstrated in Fig.2, however, little information is known about the structures of most simple ICPs because of their poor solubilty.[13]

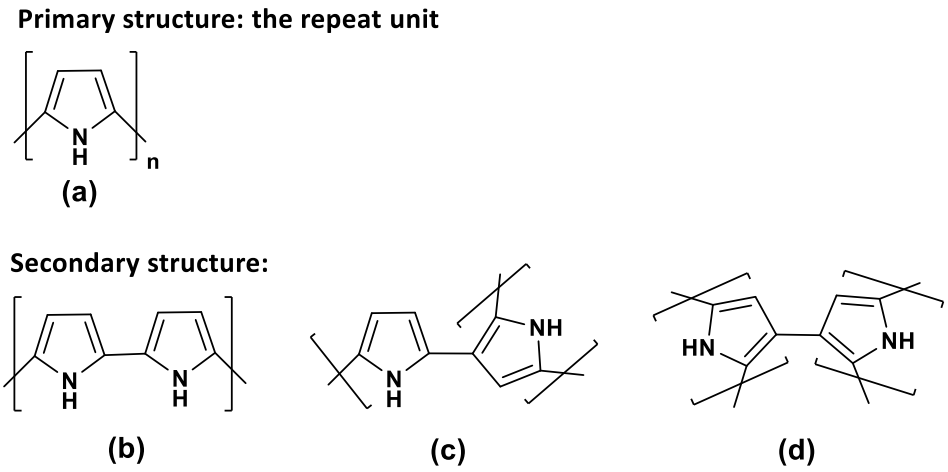

Figure 2. Structures of polypyrrole [13-15]

The big benefit of PPy is its ease of synthesis and processing in large scales to yield a large high surface area and different porosities in a wide range of solvents, including water, at room temperature.[16-19] In addition, PPy is more easily deposited than neutral pH aqueous solutions of pyrrole monomers.[20] PPy can be easily modified by covalently coupled redox groups or proteins to further enhance its functions.[21-23] Unfortunately, as a non-thermoplastic, mechanically rigid, brittle and insoluble ICP after synthesis [17,24-26], PPy is not suitable for further flexible process once synthesized.

In summary, due to the high electrical conductivity, long term environmental stability and ease of synthesis by chemical or electrochemical polymerization, PPy has a wide range of applications in chemical sensors, actuators, photovoltaic cells, electrochemical cells, and so on. [27-30]

1.1.2 Polyaniline

Although polyaniline (PANI; Fig.3) was first prepared over 150 years ago, only since the early 1980s, researchers have started to realize the value of such polymer due to the rediscovery of its high electrical conductivity.

PANI, also known as aniline black, has a variety of forms corresponding to different oxidation levels: the fully oxidized pernigraniline base, half-oxidized emeraldine base and fully reduced leucoemeraldine base, of which PANI emeraldine is a proper state with the best stability and conductivity.[6,31]

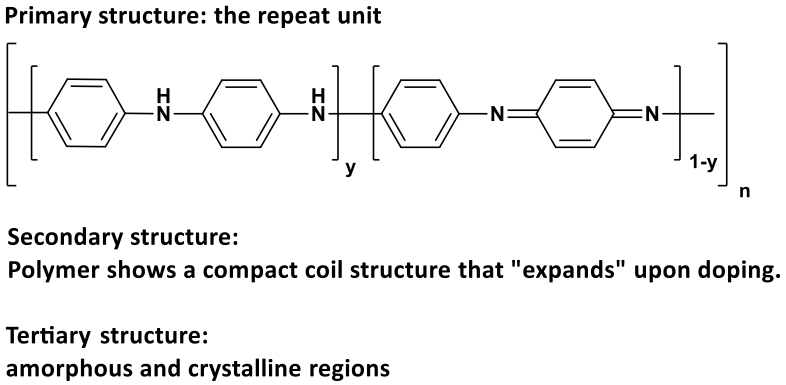

Figure 3. Structures of polyaniline [32-36]

PANI has many attractive advantages, *i.e.*, ease of synthesis in low cost, good environmental stability in addition to its capability of switching between conductive and resistive states triggered electrically. Unfortunately, the difficulty to further process, and non-biodegradability limit its applications.[37-41]

1.1.3 Polythiophene Derivatives

Most ICPs are insoluble in any solvent and infusible upon heating, which make ICPs suffer from characterizations and processing. The processability issue has been solved by introducing polythiophene (PTh), which has a long list of advantages that makes it the most suitable candidate for various applications, *e.g.*, (1) excellent conductivity larger than 100 S/cm; (2) great synthetic flexibility generating large numbers of different derivatives without decreasing the conductivity; (3) more atmospherically, thermally, chemically and electrochemically stable; (4) easier electrochemical or chemical polymerization.[42]

The mechanism of oxidative polymerization of thiophene (Fig.4) initially involves formation of oligomers, with subsequent nucleation and growth leading to a polymer material. Dimers are formed via intermediates of cation radicals at two thiophene rings;

then two such radicals dimerize to result in the formation of the bithiophene cation radical and release of two protons.

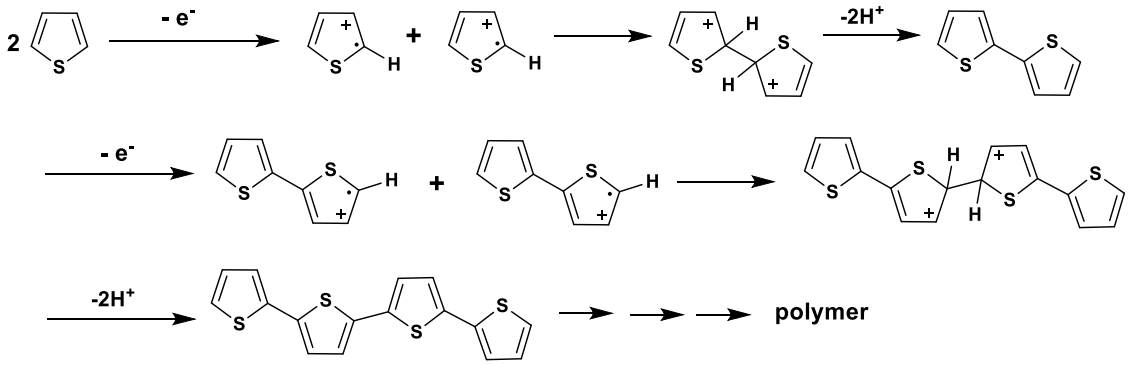

Figure 4. The mechanism of oxidative polymerization of thiophene [43]

Depending on the position of substitution on the thiophene ring at position 3 or 4 (Fig.5) and the distribution between thiophene fractions in PTh at the position 2 or 5 where two thiophene molecules are linked together, three different regioregular are initially formed, *i.e.*, head-to-tail, head-to-head, and tail-to-tail dimers. Furthermore, polymerization of the dimer generates four different, HT-HT, HT-HH, TT-HH, and TT - HT thiophene triads. This mechanism is equally applicable to other heterocycles.

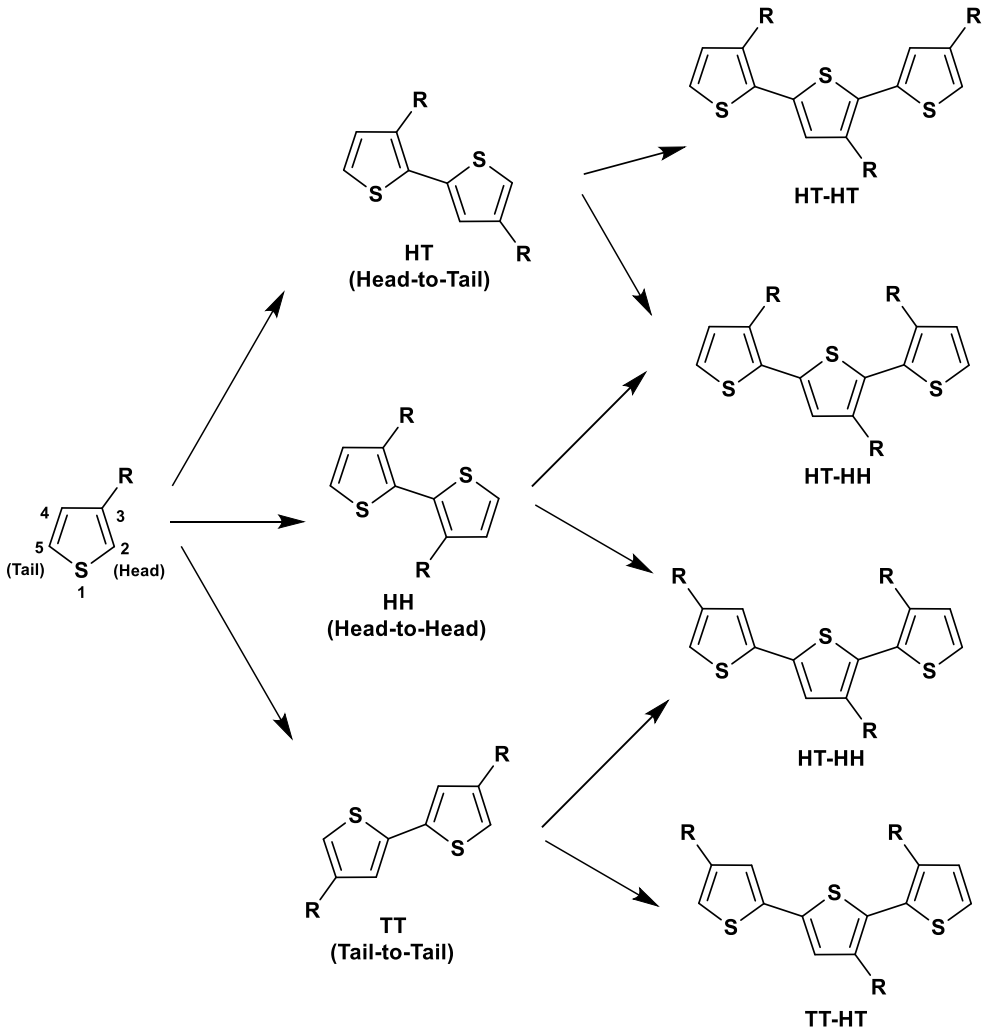

Figure 5. Structural formulas of three possible dimers and four trimers [42]

To overcome the limitation resulted from low atmospheric stability of ICPs, such as PPy and PANI, poly(3,4-ethylenedioxythiophene) (PEDOT; Fig.6) - one of the most extensively studied PTh derivatives - was first reported in 1988.[44]

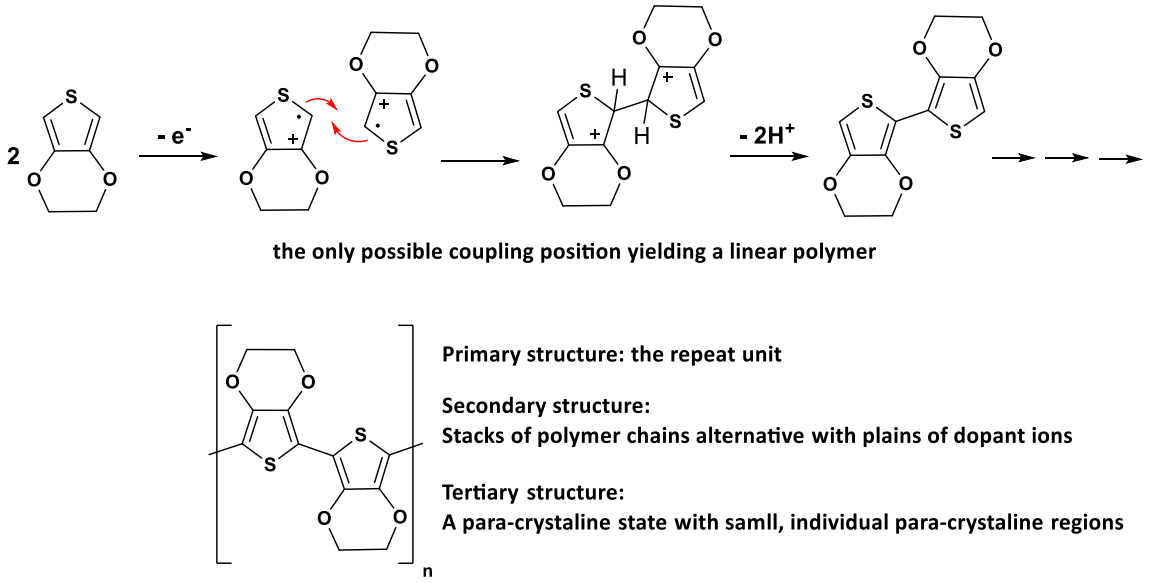

Figure 6. The mechanism of oxidative polymerization of PEDOT and structures [45]

Compared to PTh, PEDOT has a unique dioxyalkylene bridging group across the 3- and 4- positions of its heterocyclic ring, which lowers the band gap and reduction and oxidation potentials, so that its properties are greatly improved, which also prevents coupling at the 3- and 4- positions on the thiophene ring, offering a unique linear structural formula shown above. Therefore, PEDOT guarantees a better electrical conductivity, environmental and thermal stability than PPy; unfortunately, the applications of neat PEDOT are limited by its poor solubility. [6,46-47]

A solution to overcome this situation is to modify PEDOT to its composite (Fig.7). PEDOT can be dispersed and stabilized by the poly(styrene sulfonate) (PSS).[48] So far, PEDOT: PSS has been regarded as the most successful conducting polymer in practical applications.[49]

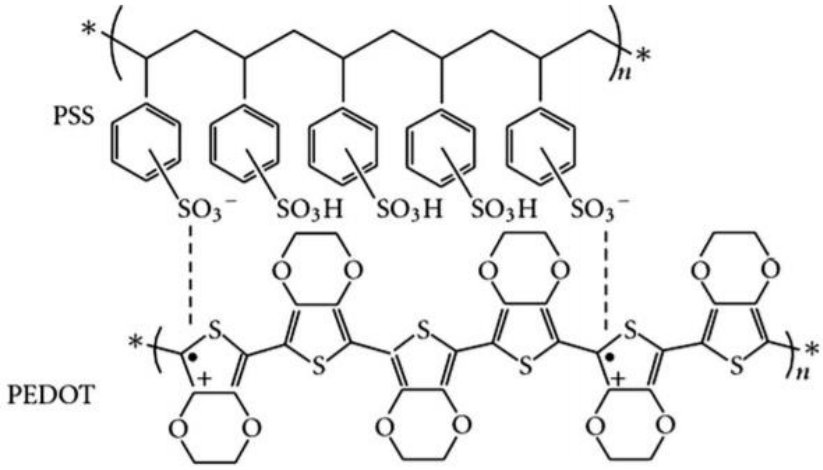

Figure 7. The structure of PEDOT: PSS

Most commonly PEDOT can be synthesized from EDOT in two methods. The first method is oxidative polymerization utilizing a chemical oxidant, which results in formation of PEDOT films. For example, poly(3,4-ethylenedioxythiophene): tosylate (PEDOT: Tos) can be synthesized using $Fe(Tos)_3$ as oxidant with reported conductivity of 4300 S/cm.[50] Recently, using patterned substrates and geometrically confined conditions, single-crystalline PEDOT nanowires have been synthesized with an electrical conductivity of 8797 S/cm.[51] Metallic behavior of the in *situ* polymerized PEDOT films has also been investigated.[52]

Conductive PEDOT films can also be formed via deposition from a stable PEDOT: PSS dispersion. Inkjet deposition of a PEDOT: PSS composite has been successfully carried out while retained its transparency, with a highly smooth surface (roughness 23-44 nm).[53] PEDOT: PSS is the only stable PEDOT dispersion commercially available in a large scale. [54]

1.2 The Source of the Conductivity

1.2.1 Conjugational Defects and Solitons

The fact that the electrons can travel within and between polymer chains results in the conductivity of doped ICPs.[31]

The combination of several factors can affect the conductivity of the ICPs. In traditional polymers, such as polyethylenes, the valence electrons have low mobility that are bound in sp^3 hybridized covalent bonds, which does not contribute to the electrical conductivity of the material. In contrast, ICPs possess a conjugated backbone of contiguous sp^2 hybridized carbon centers, *e.g.*, the ICP with the highest symmetry - polyacetylene (Fig.8), so that they are formed by conjugated double bonds.[5] Thus, ICPs are always referred to conjugated polymers, which means that the electrical conductivity is resulted from their inherent attribute, *i.e.*, alternating single and double bonds, instead of loading with external conducting particles such as metallic powders.

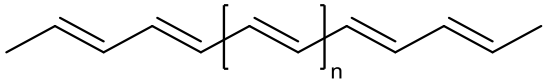

Figure 8. Structure of trans – polyacetylene

In the metallic state of polyacetylene (Fig.9), the electrons can be delocalized over the entire chain, shown as the dashed line. However, the metallic state will not actually be realized due to the long extended polymer chain and it will transform to its insulating version, forming conjugated double bonds.

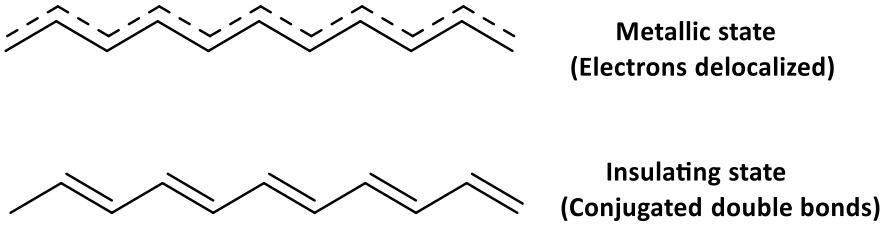

Figure 9. Metallic state and insulating state of polyacetylene

Because of the synthesis process, there will always be some conjugational defects along the chains of ICPs (Fig.10), which can be resulted from the break of a double bond into a single bond leaving a dangling bond, and which are created in pairs, named as soliton and anti-soliton.

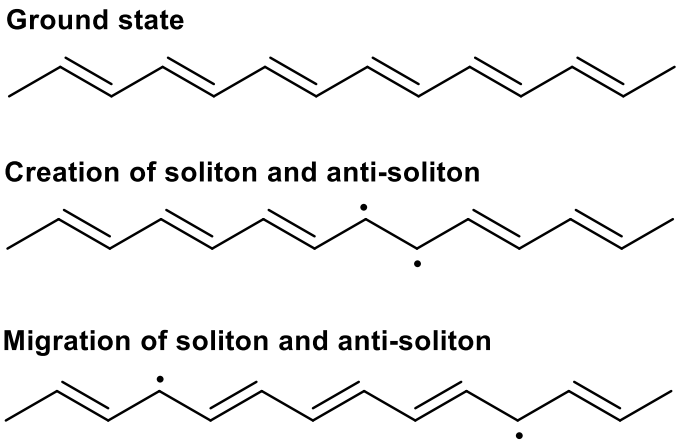

Figure 10. Creation of soliton and anti-soliton

Solitons are the particle version of solitary waves (quasiparticles), like phonons *vs.* sound waves, and photons *vs.* light waves. [55] The concept of solitary waves is derived from physicists' analytical solutions of the wave function of double - well potentials. Chemists extend this term: it is reported [56] that solitary wave solutions can be integrated in real time for the model of polyacetylene, which triggered a long discussion that reached the conclusion that the solitons phenomenon exists in polyacetylene and are responsible for its high electrical conductivity. In addition to neutral solitons, solitons can also be positive or negative: further electron removal during oxidation or electron addition during reduction likely happens at the dangling bond (Fig.11). So, in chemistry terms, the neutral soliton is a radical, the positive soliton is a carbocation and the negative soliton is a carbanion.

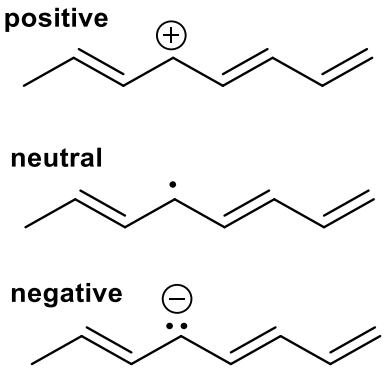

Figure 11. Neutral, positive and negative soliton, also known as carbocations, free radicals, and carbanions, respectively

1.2.2 Doping and Dopants

Despite their name, the ICPs are either insulating or semi-conducting in the neutral "undoped" form. The term "doping" in the context of ICPs is different from doping of silicon to generate semiconducting materials: the ICPs are doped up to several percent whereas classical semiconductors are in the ppm range.

Chemical doping can generate additional solitons that greatly enhance the conductivity of ICPs. Fig.12 shows the "p-doping" of polyacetylene: it begins by breaking a double bond, forming two solitons, followed by transfer of an electron from the polymer chain to the dopant so that eventually one of the solitons becomes positively charged.

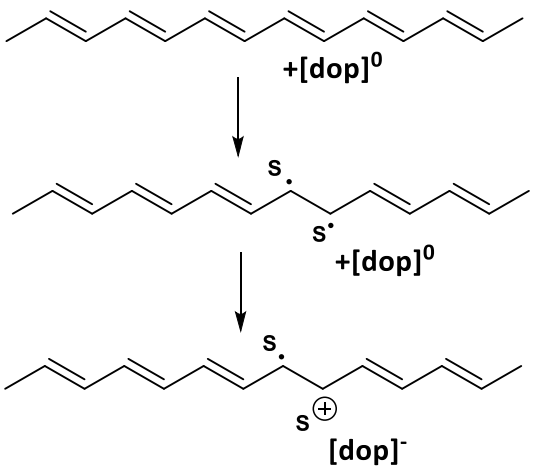

Figure 12. Creation of solitons by p-doping

In the first step a double bond is broken, followed by the transfer of an electron from the polymer chain to the dopant. Thus, two solitons are created, one neutral and the other positively charged (p-doping). The next dopant then reacts with the neutral soliton, because in most p-doping reactions stoichiometry requires the transfer of two electrons, for example: $[PA]_0 + 3I_2 \rightarrow [PA]^{++} + 2I^-_3$. However, in n-doping only one electron is transferred from dopant to the soliton on the polymer chain: $[PA]_0 + K^0 \rightarrow [PA]^- + K^-$. But in any way, very few neutral solitons survive.

As we just discussed, doping can occur in two ways: p-doping, where the polymer is oxidized and has a positive charge (stabilized by a dopant anion), and n-doping, where the polymer is reduced and possesses a negative charge (stabilized by a dopant cation). The doping process can be achieved chemically, electrochemically or via photodoping.[3,26] Generally, doping is reversible: applying electrical potential through the polymer can cause the dopant to leave or re-enter the polymer, switching between its conductive and insulating states. It is reported that there is a proportional relationship between the amount of dopant used and the conductivity of the doped ICP.[57] The conductivity can be further increased by choosing a different dopant, but this also affects the surface and bulk structural properties (*e.g.* color, porosity, volume) of the polymer.[31]

Dopants can be categorized into two types based on their molecular size: small dopants (*e.g.* Cl^-) and large dopants (*e.g.* PSS), which behave and affect the polymer differently.[7,31,58,59] Both affect the conductivity and structural properties of the polymer, but large dopants affect the material properties more dramatically, *e.g.*, increasing the density and viscosity. In addition, large dopants are more integrated into the polymer and unlikely to be leached out with time or with the application of an electrical stimulus, ensuring greater electrochemical stability. [58,59] Small dopants, on the other hand, can leave and reenter the polymer with electrical stimulation, forming the basis of the drug release applications of conductive polymers, which allows the physical properties of the polymer to be controlled through cycling between doping (oxidation) and dedoping (reduction). [31,59] A list of common doping materials for ICPs and the resultant conductivities is shown in Table 1.

Table 1. Conductivities of ICPs with selected dopants [60,61]

Polymer	Doping materials	Conductivity (S/cm)
Polyacetylene	I_2, Br_2Li, Na, AsF_5	10^4
Polypyrrole	BF_4^-, ClO_4^-, tosylate	500 - 7.5×10^3
Polythiophene	BF_4^-, ClO_4^-, tosylate, $FeCl_4^-$	10^3
Poly(3-alkylthiophene)	BF_4^-, ClO_4^-, $FeCl_4^-$	10^3 - 10^4
Poly(phenylenesulphide)	AsF_5	500
Poly(phenylene-vinylene)	AsF_5	10^4
Poly(thienylene-vinylene)	AsF_5	2.7×10^3
Poly(p-phenylene)	AsF_5, Li, K	10^3
Polyisothianaphthene	BF_4^-, ClO_4^-	50
Polyazulene	BF_4^-, ClO_4^-	1
Polyfuran	BF_4^-, ClO_4^-	100
Polyaniline	HCl	200
Poly(3,4-ethylenedioxythiophene)	poly(styrene sulfonate)	10

1.2.3 Degenerate and Nondegenerate Ground State

There are two types of ground state for the ICPs: degenerate and nondegenerate ground state. Degenerate means that the energy does not change when single and double bonds are interchanged; for nondegenerate the energy does change. Polyacetylene belongs to the first group, and all the other ICPs represent the second group. For polyacetylene, there is no difference on energy between two states that has different double and single bond arrangements (state A and state B in Fig.13), whereas for polyphenylene, the quinoidal state B has a higher energy than aromatic state A.

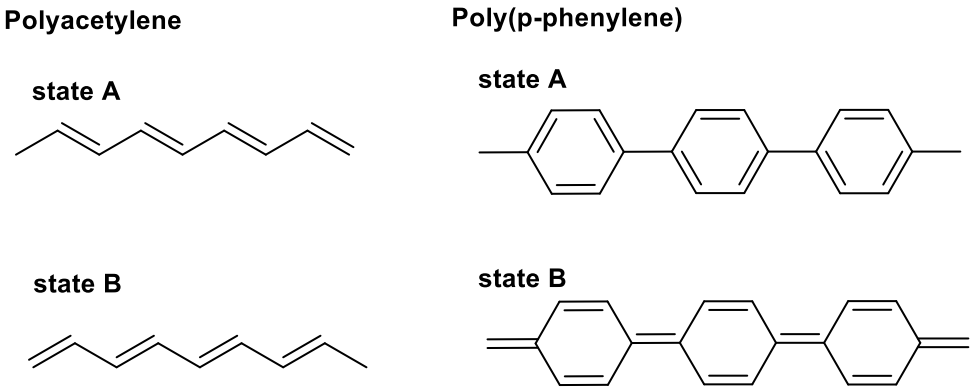

Figure 13. Degenerate (polyacetylene) and nondegenerate (poly(p-phenylene)) ground state of ICPs

1.2.4 Polaron and Bipolaron

Because of the degeneracy in polyacetylene, the position of the soliton does not matter energetically, whereas in poly(p-phenylene) the soliton is driven to move to the chain end, changing the quinoidal rings into low-energy aromatic rings and eventually it reaches a position that separates the low-energy section from a high-energy section (Fig.14). A soliton is free to move in polyacetylene, whereas in polyphenylene it is pushed to the chain end by lattice forces.

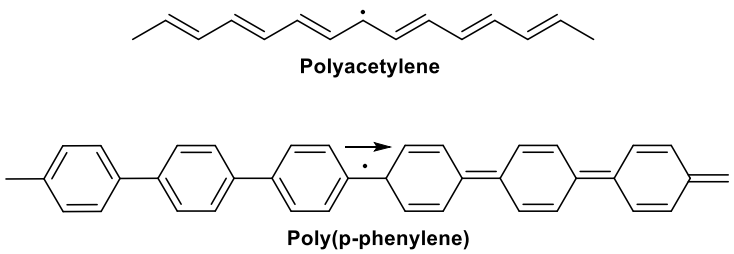

Figure 14. Solitons in polyacetylene and poly(p-phenylene)

To stabilize conjugational defects in a nondegenerate ground state of a ICP, bound double-defects must be created, which are called polarons, *e.g.*, a neutral and a positive soliton (Fig.15). The two polarons are pushed towards each other by the lattice in order to minimize the length of the quinoidal part of the chain. Generally, when two polarons meet, they immediately react: the two neutral solitons can form a bond leaving two charged

solitons called bipolarons (Fig.15), which are what are usually thought to be the dominant species involved in electron/hole mobility.

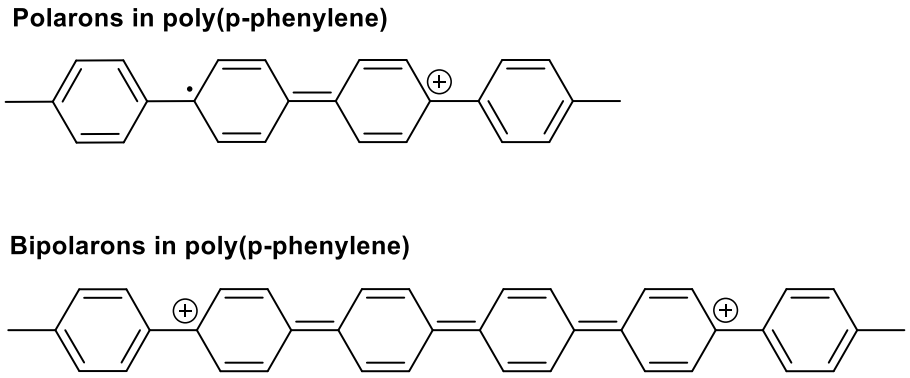

Figure 15. Polaron and bipolaron in poly(p-phenylene)

In summary, in conjugated ICPs, the p-orbitals in the series of π-bonds overlap each other to form a molecule-wide delocalized set of orbitals, allowing the electrons to be more easily delocalized throughout the molecule; the electrons have high mobility when the material is doped. Thus, the conjugated p-orbitals form an electronic band, within which the electrons become mobile when it is partially emptied.[5,31,62]

The dopant can introduce a charge carrier into ICPs by removing or adding electrons from/to the polymer chain, forming polarons or bipolarons. These additive charges can cause a relaxation of the geometry of ICPs to form a more energetically favored conformation, *i.e.* a crystal lattice distortion (Fig.16). As an electrical potential is applied, the dopants start to move in or out of a ICP, disrupting the stable backbone and allowing charge to be passed through the ICP.

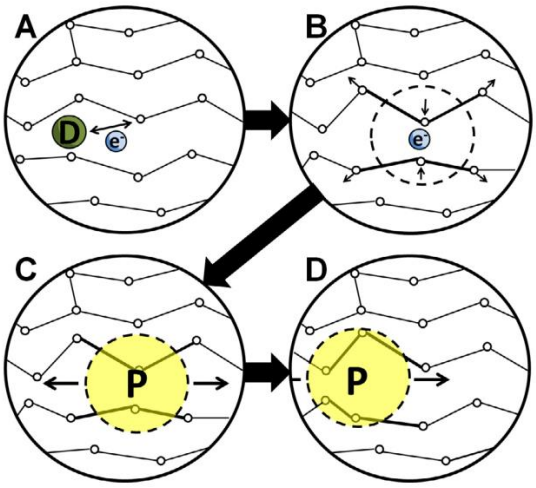

Figure 16. Illustration of conductivity of ICPs [63]

(A) The dopant removes or adds an electron from/to the polymer chain, creating a delocalized charge. (B) It is energetically favorable to localize this charge and surround it with a local distortion of the crystal lattice. (C) A charge is surrounded by a distortion, *a.k.a.* polaron (D) The polaron can travel along the polymer chain, allowing it to conduct electricity.

1.3 Synthesis and Processing

Conductive polymers may be prepared using any one of the following techniques: (1) Chemical polymerization (oxidative and nonoxidative); (2) Electrochemical polymerization; (3) Photochemical polymerization; (4) Metathesis polymerization; (5) Concentrated emulsion polymerization; (6) Inclusion polymerization; (7) Solid-state polymerization; (8) Plasma polymerization; (9) Pyrolysis; (10) Soluble precursor polymer preparation. Among those methods, chemical oxidative polymerization and electrochemical polymerization are currently the main methods for synthesizing ICPs.

Table 2. List of Polymerization Methods of ICPs [13]

Polymer	**Polymerization Method**
Polyacetylene	Chemical
Polythiophene	Chemical & Electrochemical
Polyaniline	Chemical & Electrochemical
Polyisoprene	Inclusion
Polybutadiene	Inclusion
Poly(2, 3-dimethyl-butadiene)	Inclusion
Polypyrrole	Chemical & Electrochemical
Poly(p-phenylene-terephthalamide)	Electrochemical
Poly(vinyl chloride)	Chemical
Polystyrene	Concentrated emulsion
Poly(p-phenylene)	Chemical
Poly(a-naphthylamine)	Electrochemical
Poly(1,4-phenylene)	Electrochemical
Poly(aniline-co-o-anisidine)	Chemical

The mechanisms of chemical and electrochemical oxidative polymerization of heterocycles are identical and are shown in Fig.4 for thiophene. Electrochemical oxidative polymerization uses a potentiostat to oxidize a monomer. In a typical chemical oxidative polymerization, a monomer is mixed with an oxidizing agent, *e.g.* ferric chloride ($FeCl_3$),

in solution to produce a ICP. This process can create a powder or a thick film of the polymer; [64-66] it is the most useful method for preparing large amounts of ICPs in a commercial scale, because it can be performed without electrodes.[13]

Although the conductivity of ICPs synthesized using the chemical oxidative method is generally lower than their electrochemically synthesized counterparts, [66] an additional advantage of chemical polymerization is that generally all types of ICPs can be synthesized by this technique, including some novel ICPs that cannot be synthesized by other techniques.[7]

Electrochemical polymerization has received wide attention due to its simple implementation and the advantage of obtaining a ICP in the doped state.[13] Additionally, a wider choice of cations and anions is available for use as "dopant ions" in the electrochemical polymerization process. A disadvantage of electrochemical polymerization is that it only allows the synthesis of ICPs whose monomer can undergo electrochemical oxidation, but all the main classes of ICPs currently in use, *e.g.* PPy, PANI and PEDOT, fulfil this criterion.[7]

Electrochemical polymerization is normally conducted in a cell with a standard three - electrode configuration in a supporting electrolyte dissolved in an appropriate solvent.[13] It occurs by applying a potential through electrodes placed into a solution containing the monomer of the polymer, the solvent and the electrolyte.[67-69] The three electrode cell consists of a working electrode, a counter electrode, and a reference electrode (Fig.17). The working electrode consists of a small amount of a conductive material such as platinum, typically called a button, while the counter electrode is a much larger plate of conductive material (often platinum) to allow for passage of current. A reference electrode is placed close to the other electrodes to control the electrochemical potential; the Ag/Ag^{+} reference electrode is the most commonly used reference for organic electrolyte systems. For current to flow in the electrochemical cell, a conducting medium is necessarily charged in the cell, typically an electrolyte dissolved in a polar solvent. During oxidation, the electrolyte anions balance the cations that form in the monomer and/or polymer chains, with the electrolyte cations solvated by the polar solvent.

By controlling the deposition charge and time, the temperature, the solvent, the doping agent and the electrode system,[70] the synthesized ICP films can have a wide range of properties.

In cyclic voltammetry, the potential of the electrodes is controlled, while the current varies. It protects the integrity of the component to be coated, which is recommended to obtain thin films and ideal for the manufacture of biosensors.[13,71] During cyclic voltammetry, the potential is swept between low and high potentials in cycles.[72,73] When cyclic voltammetry is used to induce polymerization of electroactive monomers, polymer is deposited from monomer solution to the working electrode.

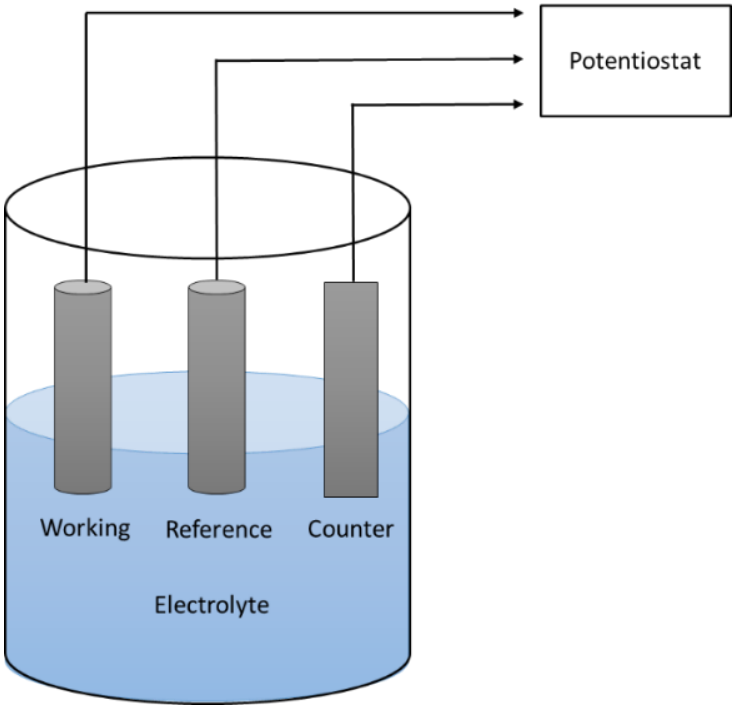

Figure 17. A schematic of the electrochemical polymerization set-up

1.4 Functionalized Graphene

1.4.1 Graphene and Characterization

Graphene (Fig.18), a monolayer sheet of sp^2-hybridized carbon in the form of a two-dimensional, atomic-scale, hexagonal lattice where one atom forms each vertex, is a fascinating material due to its extraordinary electronic, mechanical, optical and physical properties. The extended honeycomb hexagonal lattice serves as the basic building block for other important allotropes, *e.g.*, it can be stacked to form 3D graphite, rolled to form 1D nanotubes, and wrapped to form 0D fullerenes.[74]

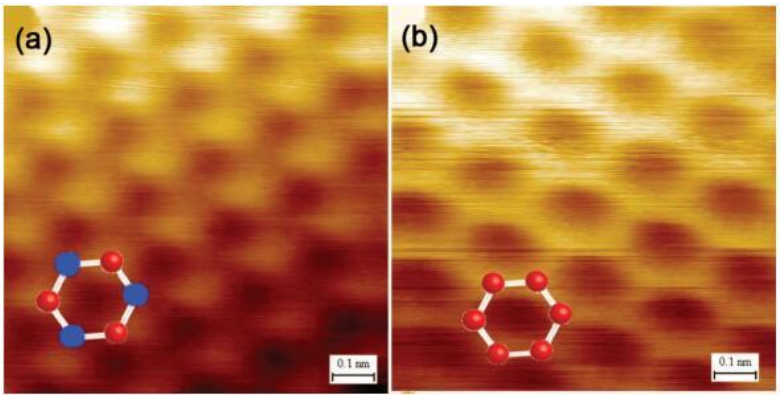

Figure 18. Scanning Tunneling Microscopy topographic images of graphene flakes [75]
(a) image of a single layer of graphene;
(b) image of the multilayer portion of the sample

Raman spectroscopy is the most common approach to probe graphene, which overcomes the disadvantages of traditional scanning probe microscopy, *e.g.*, long sample preparation time, strict substrate requirements and unreliability of confirming thickness of graphene flakes. [74, 75]

1.4.2 Motivation of Graphene Functionalization

Despite its fascinating properties and a broad range of potential applications, graphene has very poor reactivity, [76] which weakens the practical competitiveness of graphene. Single - layer graphene sheets tend to aggregate, forming irreversible agglomerates, or even restack to form graphite through π–π stacking. Functionalization

makes the fabrication of graphene sheets much easier at ambient temperature by solving the aggregation issue.[77] Graphene can be functionalized using two general methods: grafting to and grafting from. [76]

1.4.3 Common Starting Materials

(1) Graphene Oxide

One of the significant characteristics of graphene is its extensive surface originated from planar structure which can strongly immobilize guest nanoparticles. Furthermore, the oxygens of graphene oxide (GO) facilitate the nanoparticle's immobilization.

Among the methods presented to synthesize the mono layer graphene, converting graphene to GO using Hummers' method is of great interest. This method utilizes physicochemical exfoliation of graphite oxide followed by reduction of produced GO to graphene (Fig.19).

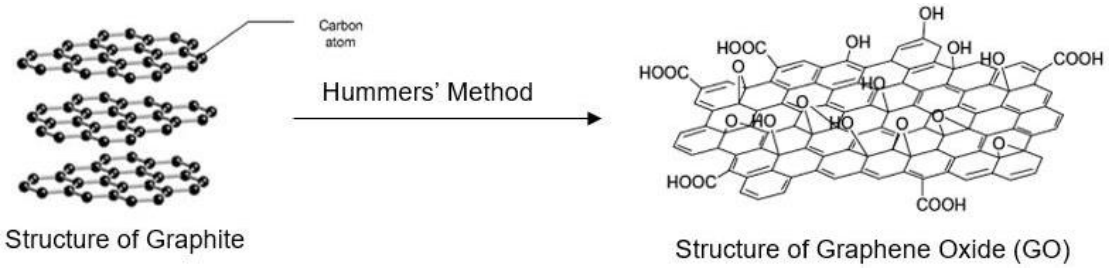

Figure 19. The schematic of GO synthesis [78,79]

(2) Humic Acid

Originally, humic acid (HA) is a soil terminology that is the organic portion contained in soil that is extractable in strong base and then precipitates in acid solution.[80] In the graphene community, HA refers to the organic material with more internal fused rings and much higher molecular weight, which is specifically extracted from Leonardite utilizing a strong base, followed by chemical reduction of the carboxylic acids of the dissolved HA (Fig.20). [80]

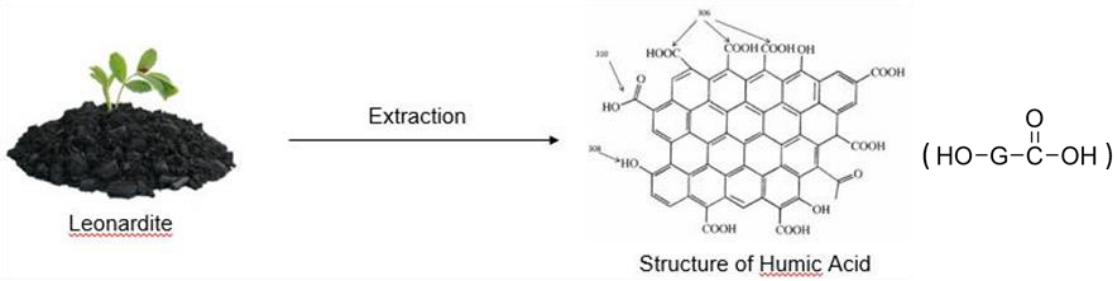

Figure 20. HA preparation from Leonardite [80]

1.4.4 Covalent Functionalization

(1) "Grafting to" method

Generally, in the grafting to method, at first chains of a polymer are synthesized. Then these pre-synthesized polymers are appended with the functional groups of GO or with its aromatic surface (Fig.21).

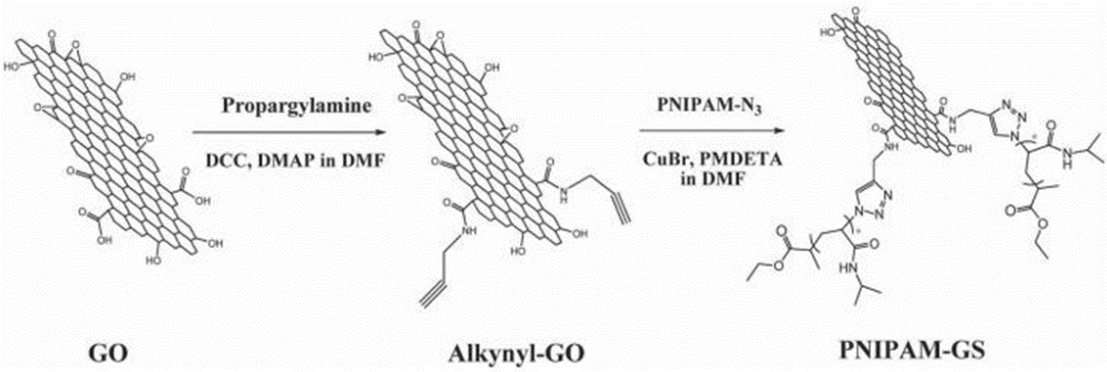

Figure 21. Functionalized graphene via "grafting to" method [81]

(2) "Grafting from" method

In contrast, the "grafting from" technique is associated with the polymerization of monomers from macroinitiators derived from the surface of graphene. These initiators are covalently attached directly to the functionalized groups of GO, or grafting the small molecules at first to bring desired functionality followed by attachment of the initiator (Fig.22).

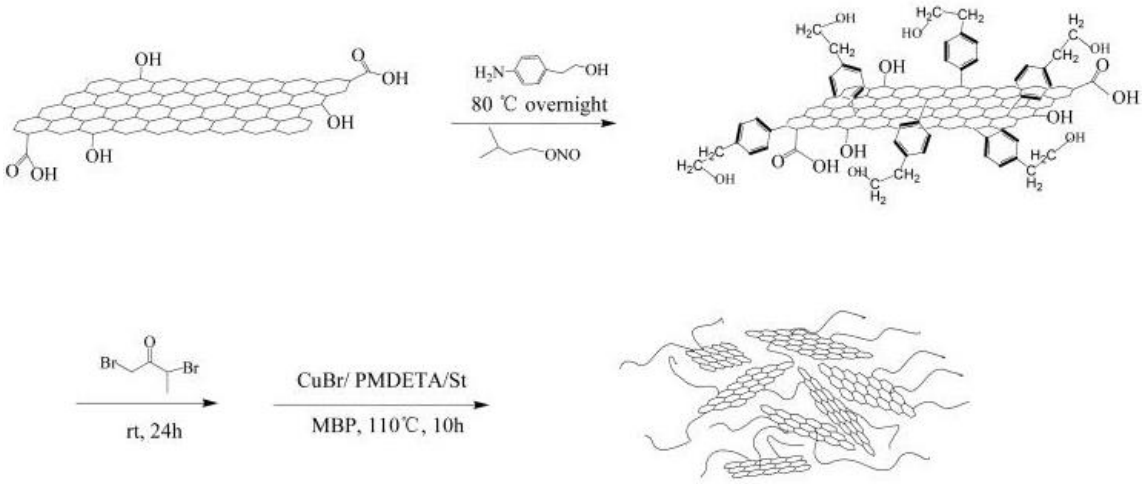

Figure 22. Functionalized graphene via "grafting from" method [82]

1.4.5 Non-Covalent Functionalization

An alternative to covalent functionalization utilizes the non-covalent interactions: π-π stacking (Fig.23) and H-bonding (Fig.24) on graphene surface. Noncovalent functionalization possesses significant advantages over covalent functionalization. While covalent functionalization results in formation of sp^3 defects on the graphene ring, non-covalent functionalization enhances the solubility without the alteration of extended π conjugation of graphene sheet.[76,83]

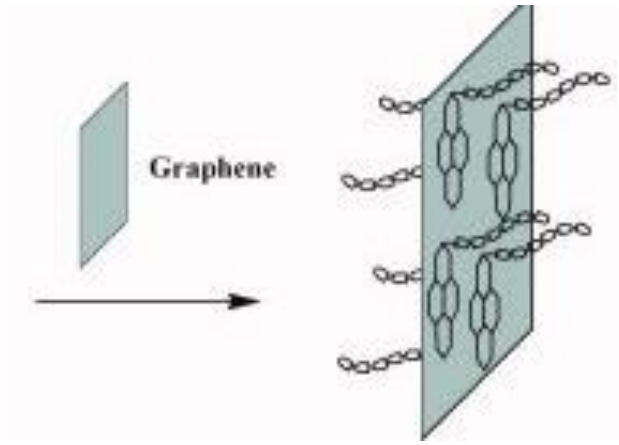

Figure 23. Functionalized graphene via π-π stacking [84]

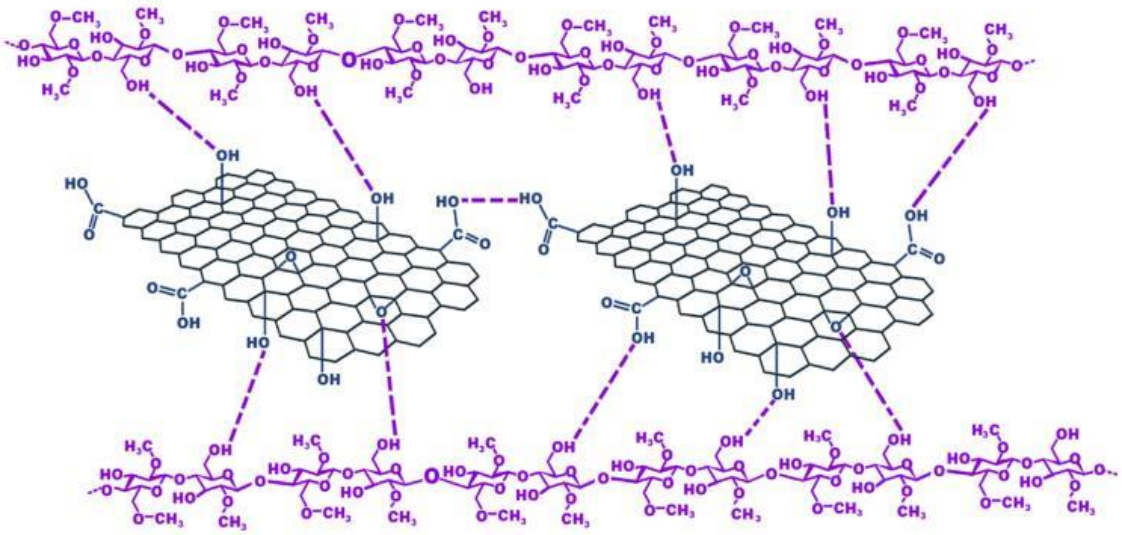

Figure 24. Functionalized graphene via H-O bonding [85]

1.5 Motivation of This Thesis

As discussed in section 1.2, ICPs depend upon conjugation (alternating single and double bonds) in the molecular structure to provide electrical conductivity along and between polymer chains. The electrical conductivity of ICPs along the length of the conjugated chain is excellent, but the electron hopping required for conduction from chain to chain results in series resistance, typically limiting the bulk ICP conductivity. For example, electron flow in typical conjugated polyacetylene chains showing a resistive gap between chains, where electron hopping is required (Fig. 25).[86]

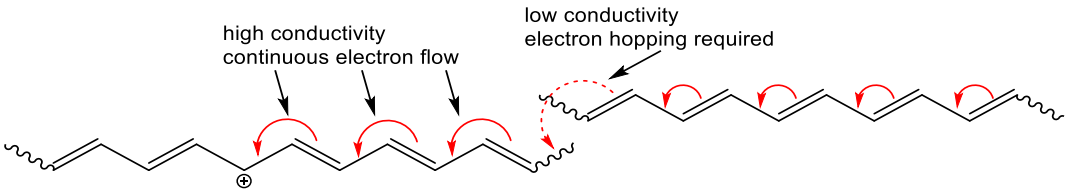

Figure 25. Electron hopping in polyacetylene

Chain-to-chain electron hopping is necessary whenever electrons reach a chain end or a defect such as a break in conjugation in the polymer chain. Minimizing the need for electron hopping should increase conductivity and improve performance of ICP-based devices. Basically, electron hopping can be minimized by increasing chain length, decreasing the number of defect sites, and providing alternative conjugated pathways within the polymer.

Several approaches have been attempted previously to provide alternative conjugated pathways. Attempt to build extra cross-linking paths from conjugated chain to conjugated chain in PEDOT using oxidative chemical vapor deposition has no enhanced conductivity than pristine PEDOT;[87] chemical cross-linking reaction that aims to crosslink poly(ethylene oxide) to the conjugated chains of PEDOT: PSS has moved little progress: only PEDOT:PSS films with lowest molecular weight PEO additives show enhanced conductivity with increasing reaction time and temperature.[88] The failures are basically resulted from the new introduced breaks in the conjugation via crosslinking.

Other efforts to achieve enhanced conductivity by incorporating composite nanostructured materials, such as carbon nanotubes, into the ICPs has had limited success,[89] but also at the expense of the polymer properties. Another additive extensively explored in ICP nanocomposites is graphene, which exhibits electrical conductivity up to 10^4 S/cm. [90] However, incorporating graphene into ICP nanocomposites typically yields conductivities of 10 - 20 S/cm compared to graphene's conductivity of 30 - 40 S/cm. [91] This is likely due to the necessity of chain hopping at the boundaries between polymer and graphene phases.

The hypothesis of this thesis is that the electron hopping can be minimized by providing alternative conjugated pathways in the ICP using a variety of polyaromatic cores (Fig.26). The aromatic core functions as a bridge that connects multiple polymer chains together to minimize the necessity for electron hopping between chains to the best extent possible. For the ICP prepared from the monomer modified with an aromatic core, when the moving electron encounters a conjugational defect, it does not have to hop to another chain; rather, it can move down another arm of the polymer, by taking advantage of the inherent polyaromatic cores (Fig.27).

Graphene is an ideal candidate for use as polyaromatic cores when preparing those functionalized ICPs. Based on the "grafting to" method, initially we need to prepare the functionalized graphene coupled with a polymer constituent, *e.g.*, EDOT. It is significant to covalently bond EDOT to graphene chemically by setting up conjugated linkages instead of mechanical method, *e.g.*, spin-coating. Then the ICP with polyaromatic cores can be prepared from polymerizing those functionalized monomers.

Due to graphene's solubility issues, it is extremely difficult to confirm the conjugated linkages by conventional characterization methods on graphene-based functionalized monomers. Therefore, a tetrafunctionalized pyrene monomer (Fig.28) is designed as a soluble alternative to the graphene-based monomer. The anticipated solubility of the pyrene-based monomer was expected to allow chemical characterization methods to be used to verify chemical structure. After confirming the feasibility of our hypothesis by exploring the pyrene model complex, the same technique can be used to prepare the ICPs with graphene-based polyaromatic cores.

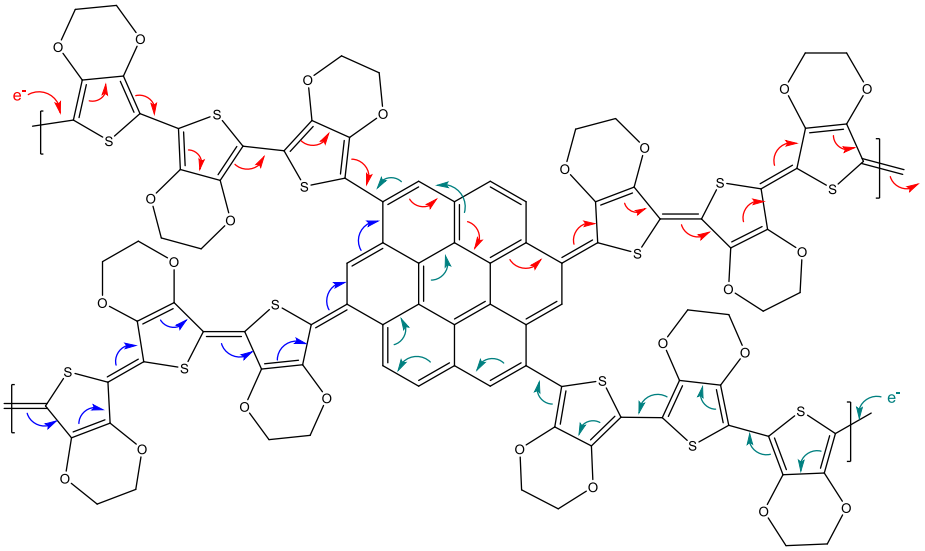

Figure 26. The schematic of the ICP monomer with an aromatic core

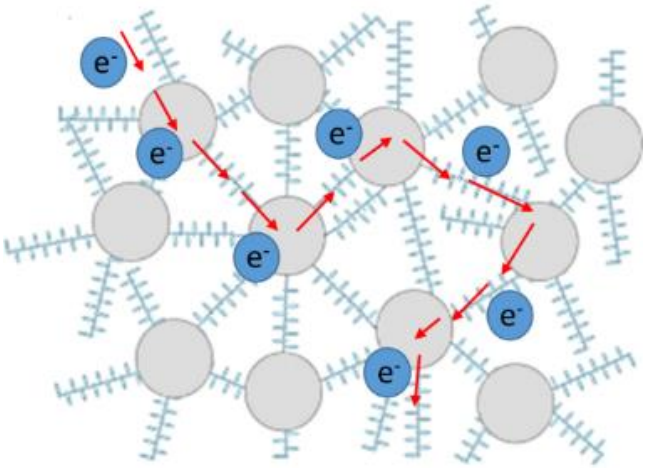

Figure 27. The schematic of the ICP with polyaromatic cores

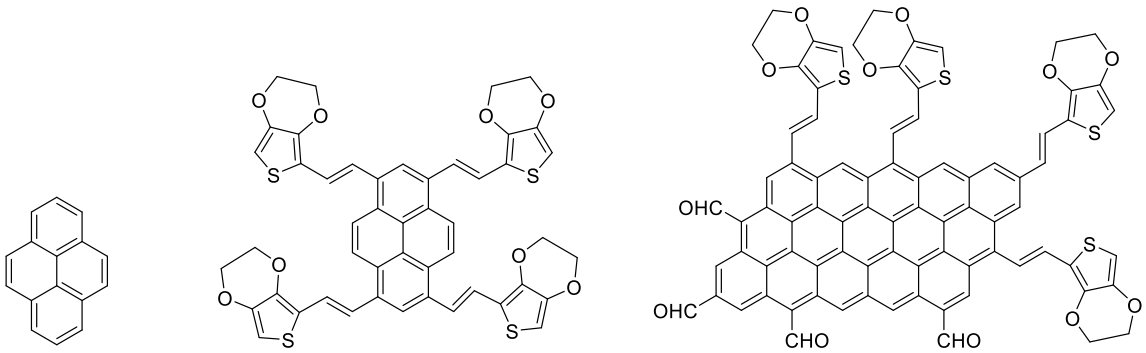

Figure 28. From left to right: structures of pyrene, tetrafunctionalized pyrene, and simplified structure of functionalized graphene

1.6 Introduction of EDOT via Vinylene Linkages

In this thesis, the coupling of pyrene and graphene matrices with EDOT is implemented via vinylene groups to ensure that the novel monomers are highly conjugated. The Wittig reaction is commonly used to synthesize alkenes from aldehydes or ketones using phosphonium ylides. A general reaction mechanism [61] is shown below (Fig.29). In the first step, a new bond is formed between the nucleophilic phosphonium ylide with the electrophilic carbonyl carbon of an aldehyde or a ketone, forming an intermediate called betaine. In the second step, the betaine collapses to a four-membered oxaphosphetane ring. In the last step, decomposition of the oxaphosphetane gives triphenylphosphine and an alkene.

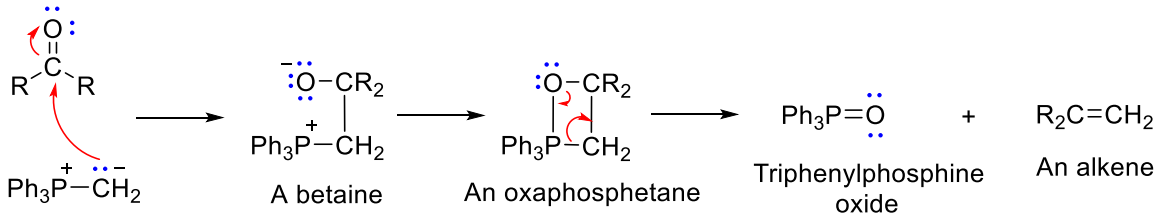

Figure 29. Mechanism of the Wittig reaction

As illustrated below (Fig.30), some Wittig reactions are Z selective, while others are E selective. As a general rule [61], those Wittig reagents with anion-stabilizing substituents, such as a carbonyl group, adjacent to the negative charge are E selective; the ylides without an adjacent anion-stabilizing group are Z selective.

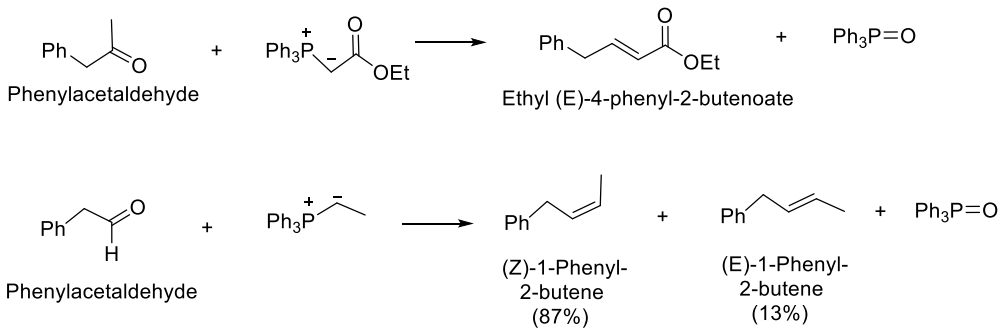

Figure 30. Examples of the Wittig reaction

Because the Wittig reaction is so useful for the preparation of alkenes, several variations of it have been explored. One of the most useful of these, known as the Horner-Wadsworth-Emmons (HWE) reaction (Fig.31) [61], uses a phosphonate ester as reagent instead of a phosphonium ylide. The particular advantage of the HWE reaction using a phosphonate-stabilized carbanion is that the resulting alkene is either entirely or almost entirely the E isomer. The big benefit of HWE reaction in this thesis is that predominant trans-linkages can increase regularity and conductivity of the ICPs, [92] Another advantage is that the by-product is water-soluble and therefore easily separated from the desired organic product.

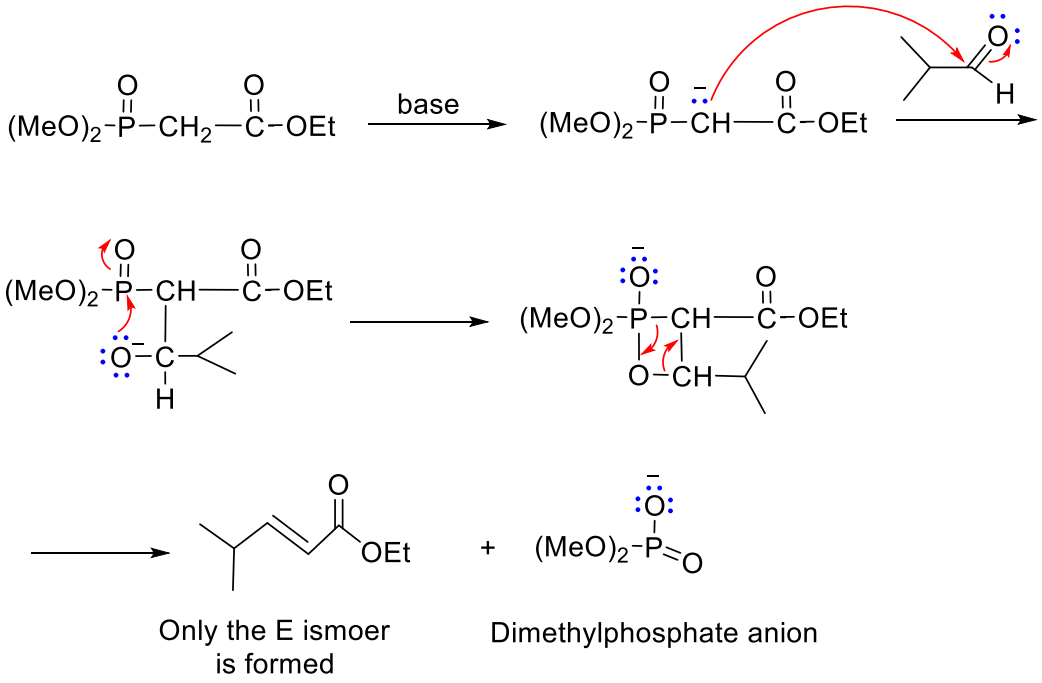

Figure 31. Mechanism of the HWE reaction

1.7 Direct Functionalization of Pyrene

Before discussing the bromination of pyrene, bromination of benzene is demonstrated (Fig.32). The Lewis acid $FeBr_3$ accepts an electron forming a new molecule $FeBr_5$ with a positive charge on Br and a negative one on Fe. One double bond on the aromatic benzene ring breaks, forming C-Br bond and a carbocation, which creates an intermediate with 3 resonance contributors. After the dissociation of hydrogen nucleus, bromobenzene is formed. Additional bromination occurs prefer entirely at the 2- and 4-positions due to resonance effects.

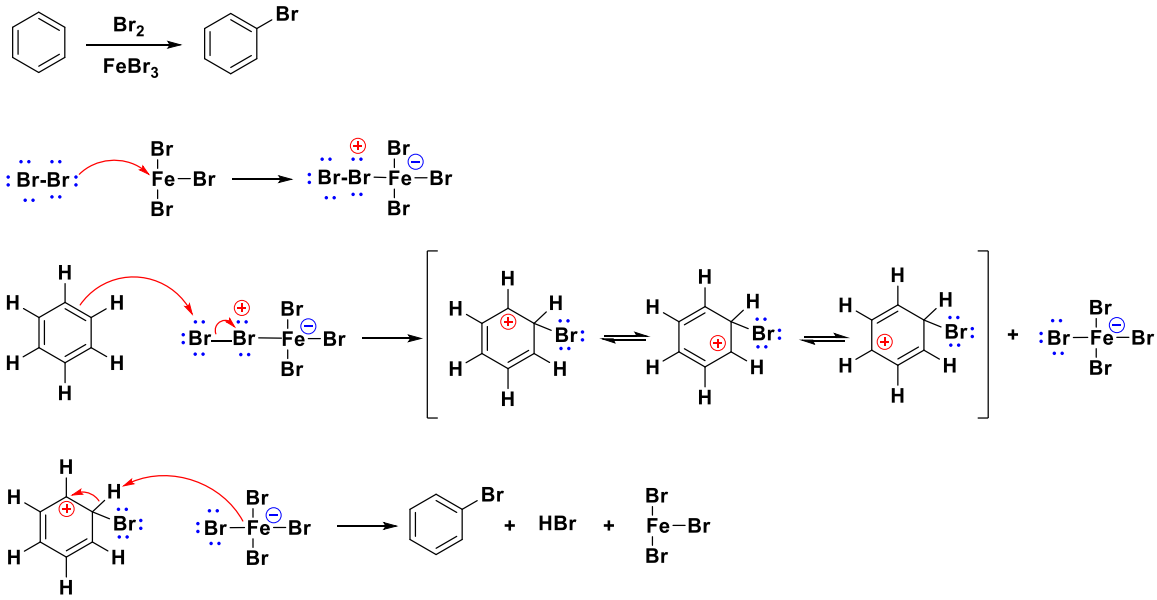

Figure 32. The mechanism of bromination of benzene

The bromination of pyrene is much more omplicated than bromination of benzene due to additional resonance contributors resulting in more possible products. Extensive research has shown that pyrene is most activated for electrophilic aromatic substitution at the 1,3,6,8- positions (Fig.33). These are the most electron-rich centers [93] and are predicted to be the most reactive by calculations on Wheland intermediates.[94] Given that the active 1,3,6,8-positions of pyrene have an equal propensity to be attached, there is a tendency for random substitution to occur, which can result in a multitude of products, the make up of which is determined by the stoichiometric ratio of the starting materials.[95] As the number of bromine atoms increases, the solubility of the bromo-substituted pyrenes decreases. The

2,7- positions of pyrene are activated towards electrophilic aromatic substitution to a lesser extent than the 1,3,6,8- positions, but they can react selectively if a very bulky electrophile is employed, *e.g.* tert-butyl chloride.[93]

Tetrabromination of pyrene has been reported previously. [97] The insoluble product was characterized using FTIR spectroscopy, indicating the presence of C-Br bonds, and using mass spectrometry, indicating tetrabromination had occurred. Further characterization to determine the position of the bromines was not possible due to poor solubility. Instead, subsequent reactions were used to produce soluble derivatives possessing the predicated 1,3,6,8- tetrasubstitution.

Pyrene has attracted much attention in organic electronics for applications. Efforts have been made in order to enhance the electronic and optical properties of pyrene derivatives by modifying its molecular structure. [96]

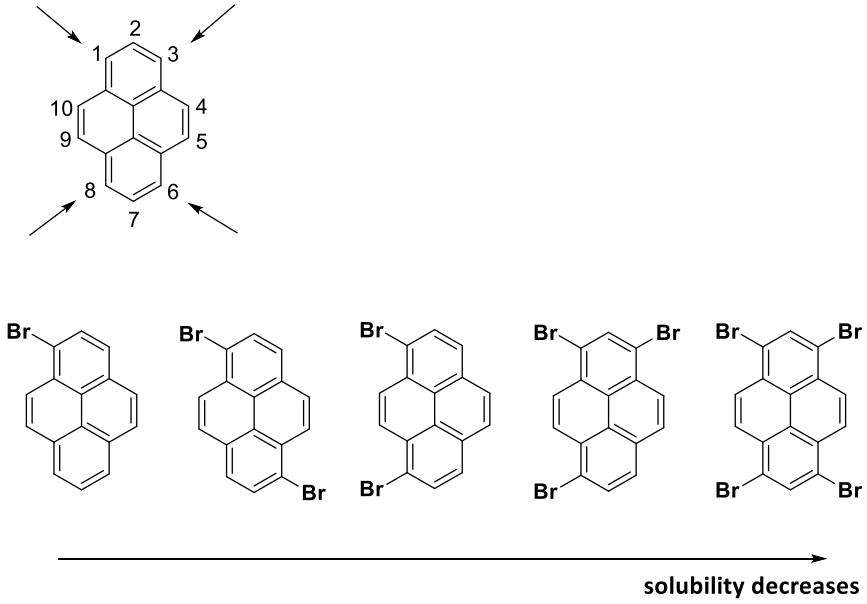

Figure 33. Structure of pyrene and bromination of pyrenes

1.8 Approach

Starting from the model compound, a tetrafunctionalized pyrene monomer (P-(V-EDOT)$_4$) has been designed and synthesized using a pyrene core coupled with EDOT via a vinylene group. Since both pyrene and EDOT are conjugated molecules, the whole novel monomer after coupling is highly conjugated. Increased conjugation is known to enhance electroactivity, lowering monomer and polymer oxidation potentials.[92]

As discussed in the previous section, the vinylene linkage can be introduced by the Wittig reaction or the HWE reaction. Considered the need for predominantly trans-linkages that increases regularity and conductivity of the ICPs, [92] the HWE reaction was adopted in this thesis (Fig. 34).

A series of purifications, *i.e.*, column chromatography and centrifugation, has been conducted before obtaining the final monomer, which has been thoroughly characterized using Fourier Transform Infrared Spectroscopy (FTIR), Proton Nuclear Magnetic Resonance (^{1}H NMR), Carbon Nuclear Magnetic Resonance (^{13}C NMR), and Two-Dimensional Nuclear Magnetic Resonance Spectroscopy (2D-NMR), including Correlation Spectroscopy (COSY-NMR) and Heteronuclear Single-Quantum Correlation Spectroscopy (HSQC-NMR).

The novel monomer P-(V-EDOT)$_4$ was first polymerized all by itself to make poly-(P-(V-EDOT)$_4$) via chemical oxidative polymerization using $FeCl_3$ as oxidant (Fig. 35); then, P-(V-EDOT)$_4$ was polymerized with additional EDOT to prepare poly-(P-(V-EDOT)$_4$ - co - EDOT) (Fig.36). Conductive measurements were carried out on those polymers compared to PEDOT (prepared via chemical oxidative polymerization from EDOT using $FeCl_3$ as oxidant) as control to explore how the polyaromatic cores and PEDOT chains affect the conductivity.

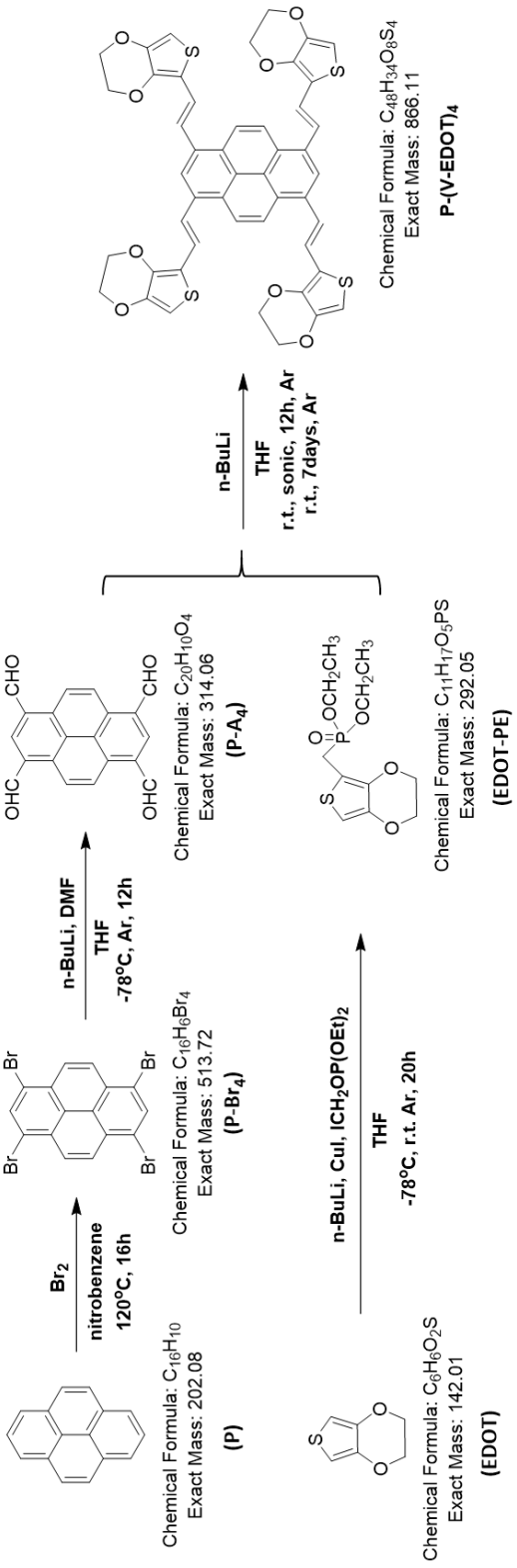

Figure 34. The synthesis route for P-(V-EDOT)$_4$

In parallel, poly-(P-(V-EDOT)$_4$) and poly-(P-(V-EDOT)$_4$ - co - EDOT) can be prepared via electrochemical polymerization and the cyclic voltammograms of those polymers can be obtained as a function of different scan rates.

The same technique can be applied to generate graphene-based hyperbranched ICPs (Fig.37). Starting from Leonardite, functionalized graphene with phenol groups on the edges (graphenol) can be readily prepared. Subsequent conversion of the benzylic alcohol groups to aldehyde groups (graphenal), is essential for the creation of conjugated linkages. Using the same reaction scheme as the model pyrene compound, the graphenal hub can be coupled with EDOT to create a hyperfunctionalized monomer (G-V-EDOT), that can be polymerized to form a highly conjugated network with enhanced conductivity.

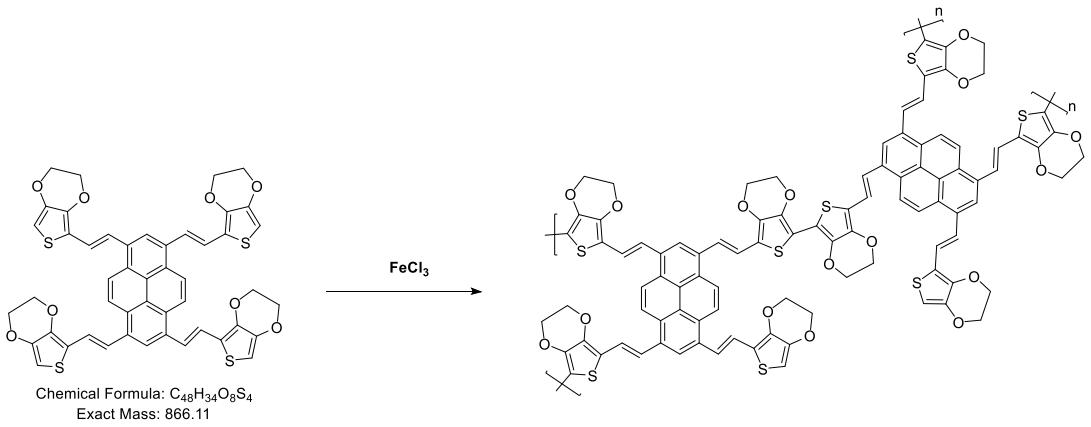

Figure 35. The synthesis of poly-(P-(V-EDOT)$_4$)

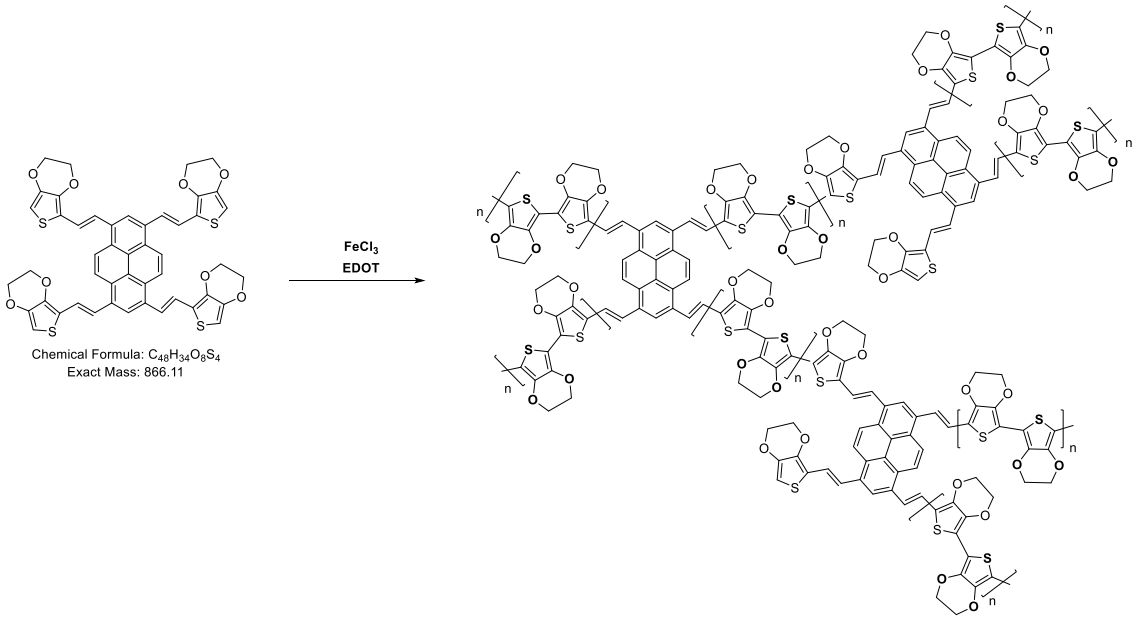

Figure 36. The synthesis of poly-(P-(V-EDOT)$_4$ - co - EDOT)

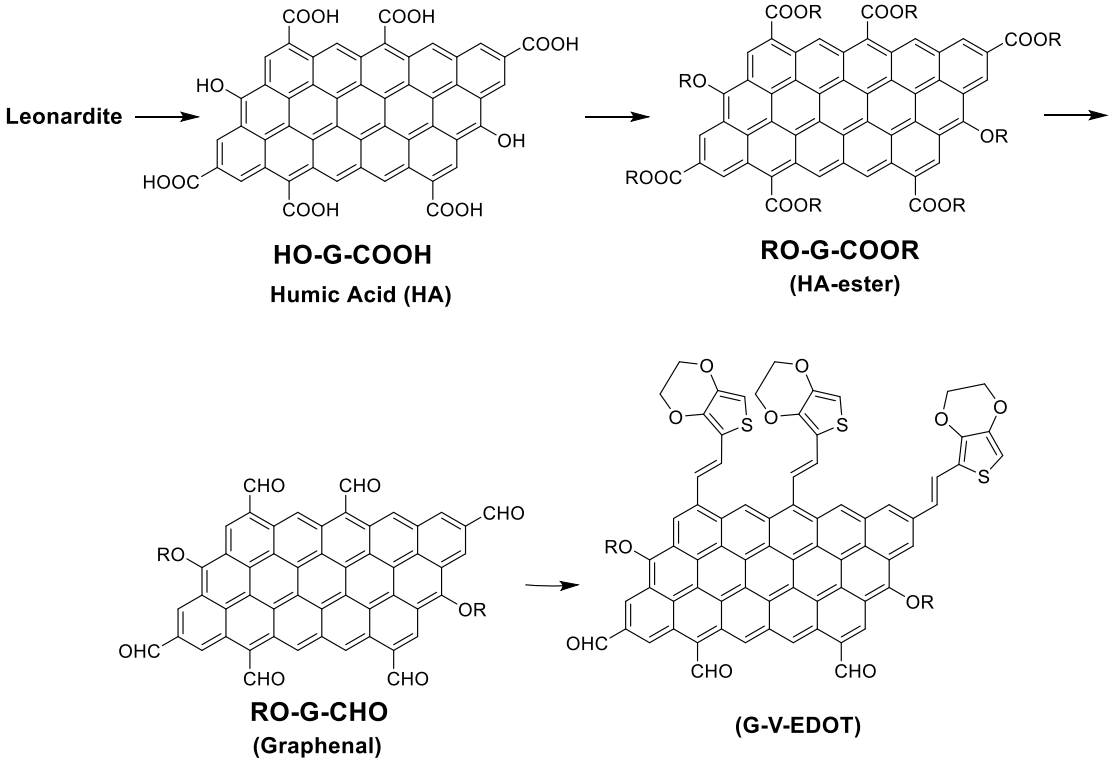

Figure 37. The synthesis of functionalized graphene monomer

(Simplified structures are used for humic acid and graphene cores)

2. EXPERIMENTAL

2.1 Materials

All reagents were commercially available and purchased from Sigma-Aldrich unless stated otherwise. EDOT was purified with 0.1M HCl followed by vacuum distillation and stored in a refrigerator prior to use.

Specifically, anhydrous THF was used for synthesis and polymerization. EDOT was further purified before using. It was dissolve in methylene chloride, extracted with 0.1 M HCl, washed with saturated sodium bicarbonate until neutral, dried over magnesium sulfate, filtered through neutral alumina, and stored in the dark in a freezer under argon. The concentration of *n*-BuLi solution in hexane was accurately measured using titration technique. [98]

2.2 Instruments and Procedures

2.2.1 NMR

All soluble compounds related to the research were characterized with NMR, as well as P-A_4 and P-(V-EDOT)$_4$ monomers with limited solubility.

NMR characterization were conducted using the Bruker 500Hz NMR spectrometer provided by Department of Chemistry & Biochemistry, Texas State University. A set of values of number of scans (NS) is applied to different types of NMR spectroscopy: ^{1}H NMR (NS = 1024 for P-(V-EDOT)$_4$; NS = 16 for other organic compounds), ^{13}C NMR (NS =1024), COSY-NMR (NS = 2048), HSQC-NMR (NS = 2048).

Figure 38. Bruker 500MHz NMR spectrometer

2.2.2 FTIR

All insoluble compounds of functionalized pyrene and graphene compounds were characterized using FTIR spectroscopy.

FTIR characterization utilized a Bruker Tensor II FTIR spectrometer provided by the Department of Chemistry & Biochemistry, Texas State University. The main parameters are listed below:

- Load method: MIR_DTGS.xpm;
- Resolution: 2 cm^{-1};
- Number of scans: 16;
- Wavelength range: 400 – 4000 cm^{-1};

Samples were pressed with KBr powder (300mg KBr: 10mg sample) to prepare the FTIR pellets used for characterization.

Figure 39. Bruker Tensor II FTIR spectrometer

2.2.3 Conductivity Measurement

Conductivity measurements were performed on PEDOT, poly-(P-(V-EDOT)$_4$) and poly-(P-(V-EDOT)$_4$ - co - EDOT) using the four-point collinear probe provided by Analysis Research Service Center, Texas State University. To simplify measurements, a single instrument, the Model 2450 SourceMeter® Source Measure Unit Instrument can be used, which provides the source current and measures the voltage. Sample pellets were prepared by compressing 200mg of each sample in a die. Sample thicknesses were measured using a micrometer. Measurement parameters are listed below.

Sweep type: linear;
Start current: - 0.01A;
Stop current: 0.01A;
Step current: 0.0002A;
# of steps: 101;
Current range: 10mA;
Voltage limit: 5V;
Delay: 0.1s.

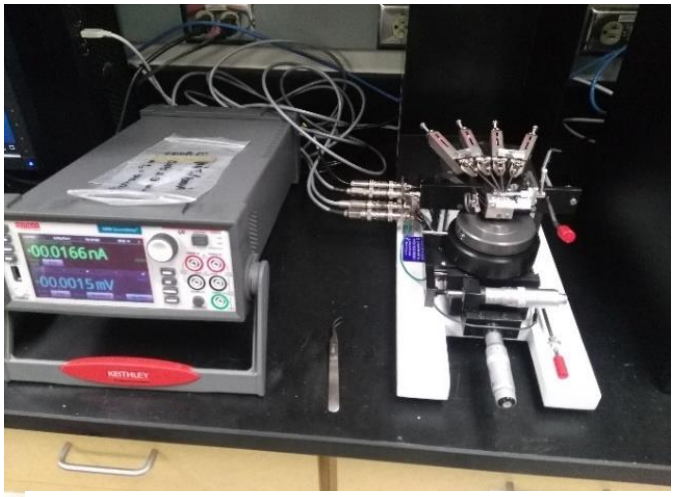

Figure 40. Four-point collinear probe instrument

2.2.4 UV-VIS

UV-VIS spectra were obtained using a PerkinElmer Lambda 365 spectrometer provided by Department of Chemistry & Biochemistry, Texas State University. Sample solutions (P, P-Br_4, P-A_4, and P-$(V\text{-}EDOT)_4$) were prepared in THF and were placed in glass cuvettes. The absorbance of each sample were acquired from 200 - 700 nm.

Figure 41. UV-VIS spectrometer

2.3 Synthetic Methods and Characterizations

2.3.1 1,3,6,8-Tetrabromopyrene Synthesis

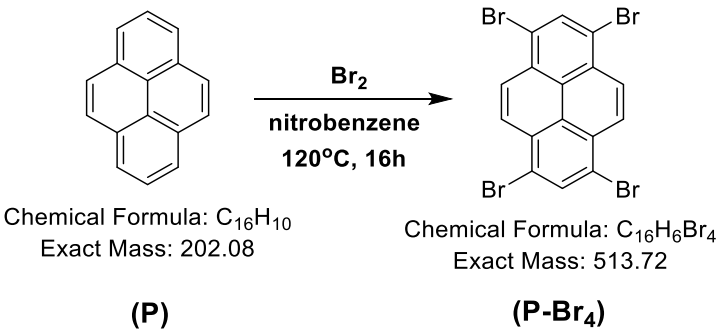

Figure 42. Synthesis of 1,3,6,8- tetrabromopyrene

To a three-neck flask charged with pyrene (1eq, 2g, 10mmol) and 70mL of nitrobenzene, bromine (4.5eq, 7.2g, 45mmol) in 20mL of nitrobenzene was added dropwise at 80℃. The resulting yellow suspension was stirred at 120℃ for 16h. After cooling down to the room temperature (room temperature), the suspension was filtered giving dark yellow solid, washed with EtOH to yield a pale gray solid that was dried in vacuo for 3h with 90% yield.

FTIR (A.2) 3445.73, 3078.14, 1923.46, 1742.39, 1631.82, 1592.18, 1465.96, 1452.77, 1384.33, 1357.60, 1290.47, 1266.46, 1227.36, 1055.34, 980.66, 873.84, 811.41, 691.13, 674.71, 495.57 cm^{-1}.

Literature [97] reported FTIR characteristic peaks are 1590, 1464, 1452, 1226, 1053, 986, 872, 810, 690, 673 cm^{-1}.

2.3.2 1,3,6,8-Pyrene tetracarbaldehyde Synthesis

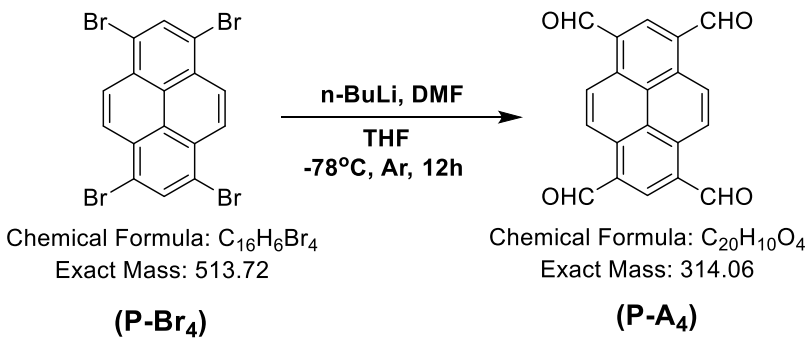

Figure 43. Synthesis of 1,3,6,8-pyrene tetracarbaldehyde

The synthesis method was adapted from the literature reporting a similar compound. [99] P-Br_4 (1eq, 2.22g, 4.32mmol) was dissolved in THF (200mL) and cooled to -78 ℃ under Ar, showing as a yellow suspension. After 30mins, *n*-BuLi (2.5M in hexane solution, 30eq, 130mmol, 52mL) was added dropwise and the resulting suspension was stirred for 4hrs, during which the color changed to orange. DMF was added and the mixture continued to stir for 4hrs at -78 ℃ and additional 2 days at room temperature with the suspension became more transparent. A dark red precipitate formed when 75mL of saturated NH_4Cl was added. Filtration yielded the product as orange solid with 80% yield.

^{1}H NMR (500 MHz, THF-d8) δ 10.96 – 10.72 (m, 4H), 9.78 – 9.66 (m, 2H), 8.98 – 8.75 (m, 4H) (A.3).

FTIR: 3443.36, 3075.46, 3041.09, 2877.14, 2752.47, 1682.41, 1597.88, 1578.36, 1559.43, 1481.14, 1384.24, 1232.68, 1194.40, 1151.43, 1004.23, 927.95, 916.14, 903.94, 849.71, 830.55, 808.77, 702.02, 499.87 cm^{-1} (A.4).

2.3.3 EDOT Phosphonate Ester Synthesis

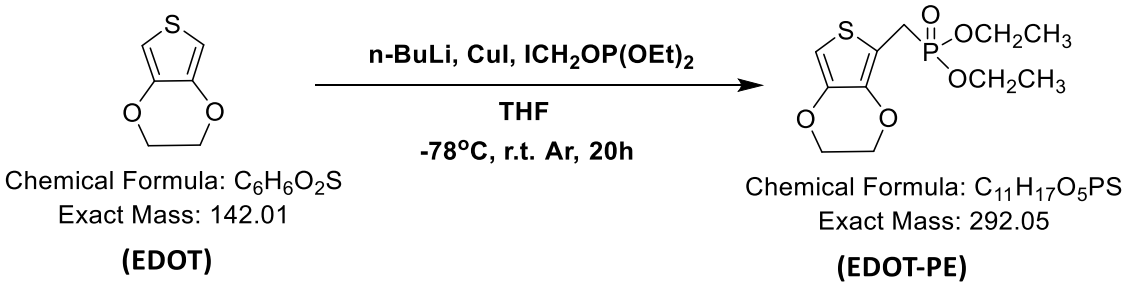

Figure 44. Synthesis of EDOT phosphonate ester

To a solution of EDOT (1eq, 3.55g, 25mmol) in dry THF (75mL) at -70℃ under Ar, *n*-BuLi in hexane (1eq, 25mmol) was added dropwise. The resulting solution was stirred for 1 h. The solution was added to a Schlenk flask charged with dry CuI (1eq, 25mmol, 4.75g), via cannula, at -50 ℃. After stirring for additional 1 h at -20℃, diethyl-iodomethylphosphonate (1eq, 25mmol, 6.95g) was added. The mixture was stirred at room temperature for 7 days. The mixture was extracted with EtOAc and H_2O. It was purified by column chromatography (EtOAc / petroleum ether = 1: 1 -> EtOAc) [100] , and evaporated to yield a brown oil product with 40% yield.

^{1}H NMR (400 MHz, $CDCl_3$) δ 6.18 (d, J = 0.9 Hz, 1H), 4.16 (d, J = 6.1 Hz, 4H), 4.11 – 4.04 (m, 4H), 3.18 (dd, J = 20.2, 1.9 Hz, 2H), 1.30 – 1.25 (m, 6H) (A.8).

Literature [100] : ($CDCl_3$) d 6.20 (d, 1H, $^5J_{H-P}$ = 2.8 Hz); 4.18 (m, 4H); 4.10 (m, 4H); 3.20 (d, 2H, $^2J_{H-P}$ = 20 Hz); 1.30 (t, 6H, $^3J_{H-P}$ = 7.0 Hz).

2.3.4 Tetrafunctionalized Monomer Synthesis

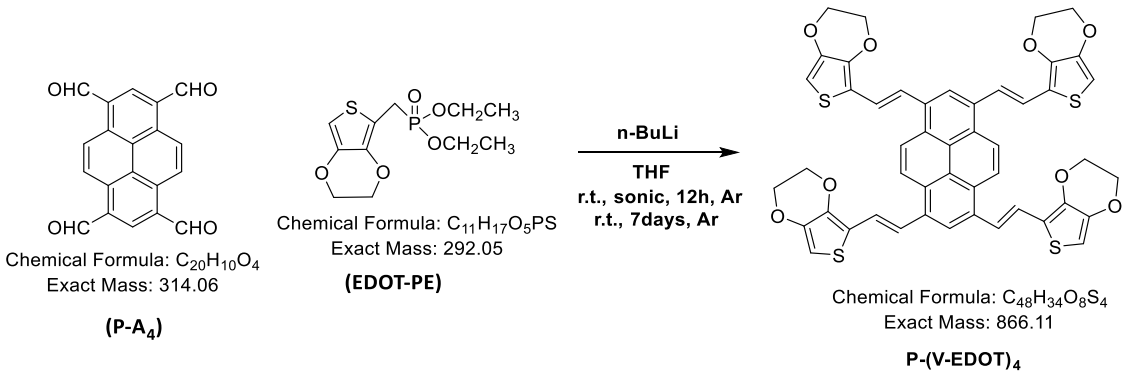

Figure 45. Synthesis of the tetrafunctionalized monomer

The synthesis method was adapted from the literature reporting a similar compound.[100,101] To a Schlenk flask charged with P-A_4 (1eq, 36mg, 0.1156mmol) and EDOT Phosphonate Ester (8eq, 270mg, 0.9245mmol), *n*-BuLi in hexane (8eq, 0.9245mmol) was added dropwise at room temperature under argon. The mixture was sonic activated for 2 h and the suspension was stirred at room temperature for 7days. After evaporating the solvent, washed the dark red solid with MeOH/H_2O (v/v 1:1).[100,101] Centrifuge yielded a red brown solid that was dried in vacuum for 3hrs. The yield was ca. 50%.

^{1}H NMR (500 MHz, THF-d8) δ 7.13 (d, J = 8.5 Hz, 4H), 6.83 (d, J = 8.8 Hz, 2H), 6.41 (d, J = 15.8 Hz, 4H), 6.14 (s, 4H), 6.00 – 5.91 (m, 4H), 4.18 (dd, J = 21.1, 4.6 Hz, 16H)

FTIR: 3432.47, 3106.9, 2962.40, 2921.75, 2870.36, 1595.73, 1482.01, 1437.83, 1384.38, 1365.15, 1261.43, 1166.20, 1068.79, 957.90, 905.15, 803.01, 710.91, 674.84, 465.46 cm^{-1} (A. 11)

2.3.5 Poly-(P-(V-EDOT)$_4$) Synthesis

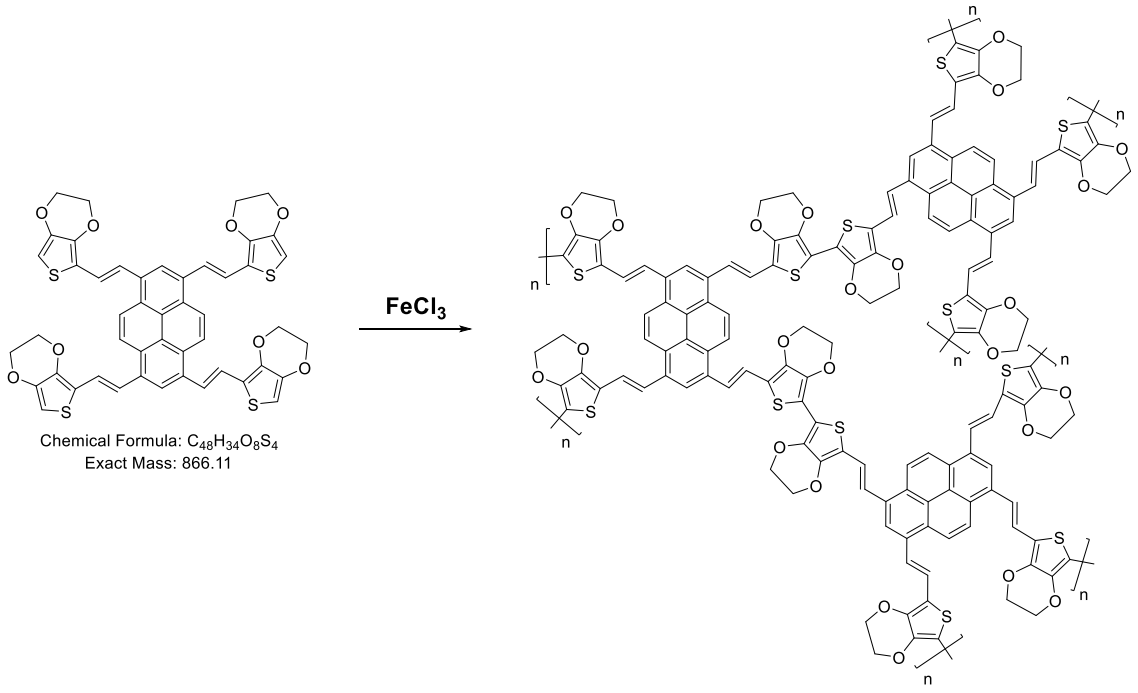

Figure 46. Synthesis of poly-(P-(V-EDOT)$_4$)

P-(V-EDOT)$_4$ (1eq, 100mg, 0.1155mmol) and THF (50mL) were combined together to form an orange suspension, from which a suspension of $FeCl_3$ (20eq, 2.31mmol, 370mg) in THF (20mL) was added. The resulting suspension was stirred at room temperature for 24h. The black solid was removed via filtration, washed with MeOH and H_2O, and dried in vacuum oven for 3h. The yield was 75%.

2.3.6 Poly-(P-(V-EDOT)$_4$ - co - EDOT) Synthesis

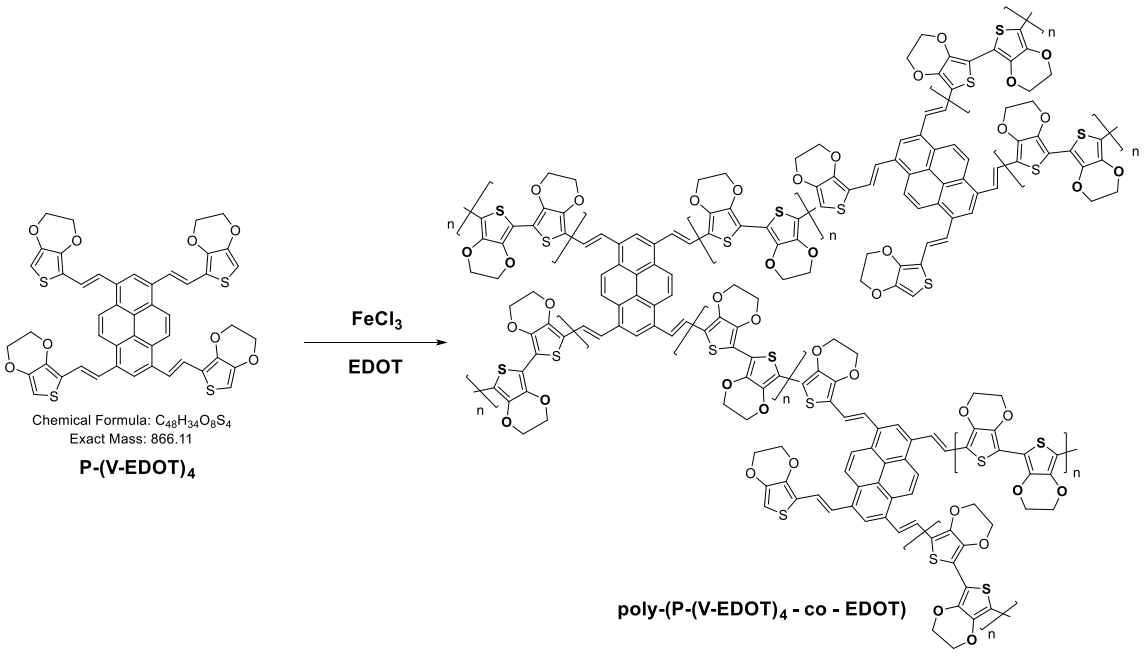

Figure 47. Synthesis of poly-(P-(V-EDOT)$_4$ - co - EDOT)

P-(V-EDOT)$_4$ (1eq, 100mg, 0.1155mmol) and THF (50mL) were mixed together to form a suspension in orange, to which a suspension of $FeCl_3$ (20eq, 2.31mmol, 370mg) in THF (20mL) was added. EDOT (10eq, 1.155mmol, 164mg) in $CHCl_3$ (20mL) was added quickly. The resulting suspension was stirred at room temperature for 24h. The black solid was removed via filtration, washed with MeOH and H_2O, and dried in vacuum oven for 3h. The yield was 85%.

2.3.7 PEDOT Synthesis

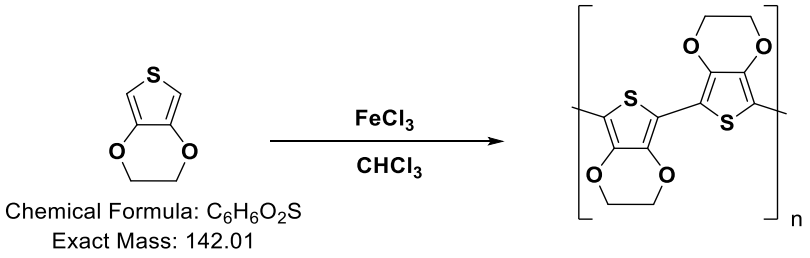

Figure 48. Synthesis of PEDOT

A solution of EDOT (1eq, 500mg, 3.52mmol) in $CHCl_3$ (5mL) was quickly added to a solution of $FeCl_3$ (4eq, 14mmol, 2.25g) in $CHCl_3$ (30mL). [102] The color of the solution changed from orange to black. The resulting solution was stirred at room temperature for 24h. The black solid was removed via filtration, washed with MeOH and H_2O and dried in vacuum oven for 3h. The yield was 90%.

3. RESULTS AND DISCUSSION

3.1 NMR Spectra Analysis

In the ^{1}H NMR spectrum of P-(V-EDOT)$_4$ (Fig.49), the intensity of the signal of the complex is weak due to its limited solubility in solvent (it forms a suspension in THF and is insoluble in common organic solvents), compared to the solvent peaks. However, those signal peaks are still readable for identification.

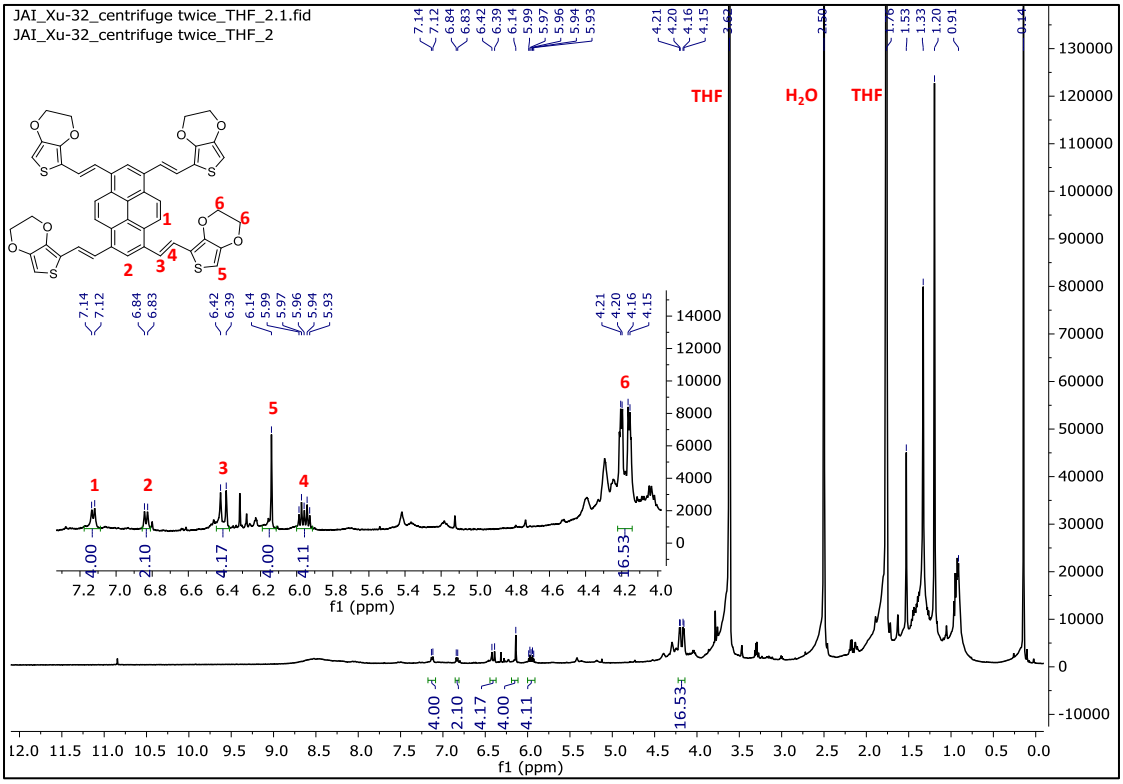

Figure 49. ^{1}H NMR spectrum of P-(V-EDOT)$_4$

The chemical shifts and integrals of all the characteristic peaks are consistent with the expectation based on the structure of the complex. The two types of protons on the aromatic pyrene ring (#1 & #2) correspond to two doublets at 7.14 and 7.12ppm, 6.84 and 6.83ppm, respectively. The peaks corresponding to two vinylene protons, *i.e.*, trans-vinylene (#3 & #4), which are used to connect pyrene ring and EDOT as a conjugated linkage, can be seen as the most significant indication to predict whether the coupling

reaction happens, correspond to a doublet at 6.42ppm and 6.39ppm, and a multiplet at around 5.95ppm. A strong singlet at 6.14ppm corresponds to the only proton on the thiophene ring (#5). The chemical shifts of the four protons (#6) on the heterocyclic ring are 4.15ppm, 4.16ppm, 4.20ppm and 4.21ppm, which only are similar to the chemical shift observed for pure EDOT at 4.18ppm, as well as EDOT-PE at 4.15ppm and 4.17ppm.
Peaks appearing from 0.7 ppm to 1.7 ppm are probably due to the impurities, *e.g.*, excess EDOT phosphonate ester, resulted from manipulation of filling NMR test tube using samples directly from centrifugation tube, where a bit of EDOT phosphonate ester solution in MeOH left. A more decent ^{1}H NMR spectrum can be obtained using samples treated with multiple centrifugation.

The 2D-NMR further confirms the structure. In the COSY-NMR (Fig.50), obviously, the correlation between two protons on the pyrene ring (#1 & #2) can be observed, and particularly the correlation between two protons on the trans vinylene linkage (#3 & #4), which is a strong evidence showing that the EDOT has been successfully linked to the pyrene backbone via conjugated bonds that meets the essential guideline of the designed monomer of the ICP with an aromatic core.

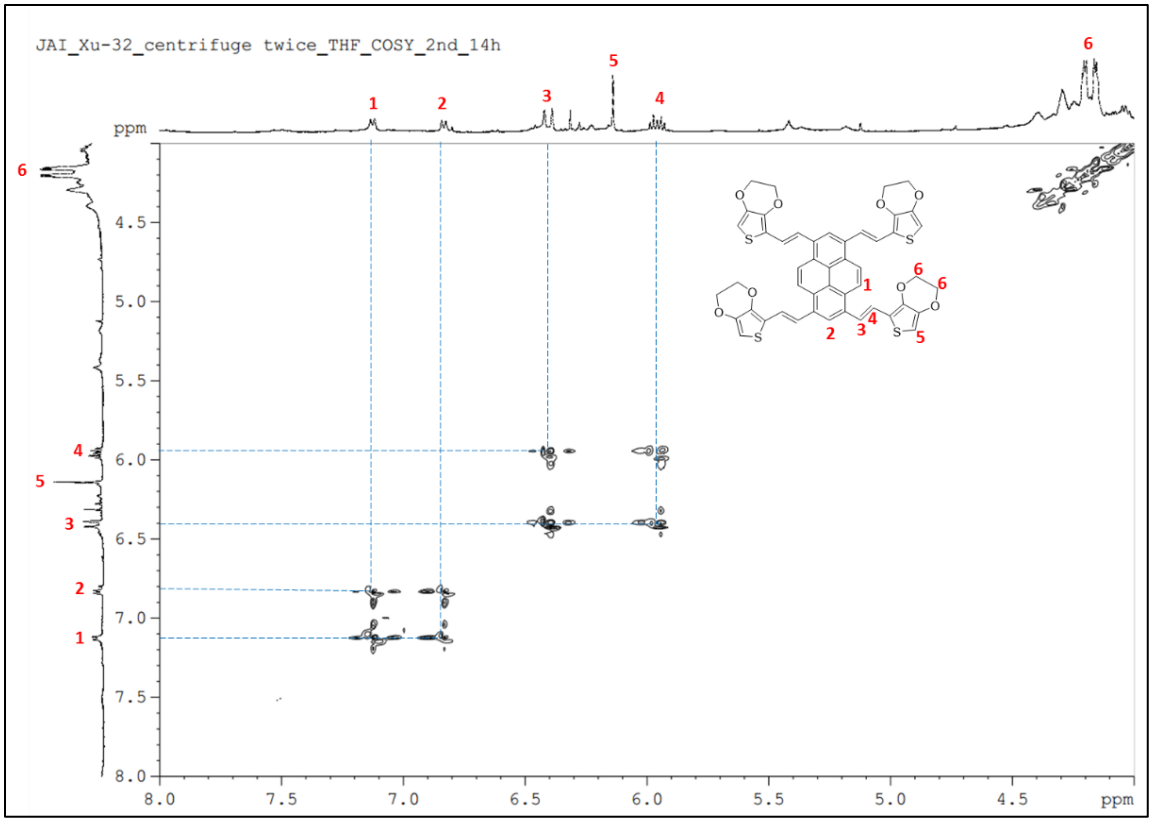

Figure 50. COSY-NMR spectrum of P-(V-EDOT)$_4$

Due to solubility issues, the ^{13}C NMR spectrum of P-(V-EDOT)$_4$ was difficult to interpret (A.9), even after 1024 scans. However, collaborated with HSQC-NMR spectrum (Fig.51), which is used to assign ^{13}C chemical shifts based on correlation with the ^{1}H chemical shifts (Fig.49). Interpretation of HSQC-NMR spectrum mainly involves the observation of correlation between each proton peaks on ^{1}H NMR spectrum and carbon peaks on ^{13}C NMR spectrum. For instance, based on the correlation with #5 proton, it can be predicted that the #10 carbon corresponds to the carbon on the thiophene ring. Using the same method, all the carbons on the ^{13}C NMR spectrum of the tetrafunctionalized monomer can be assigned.

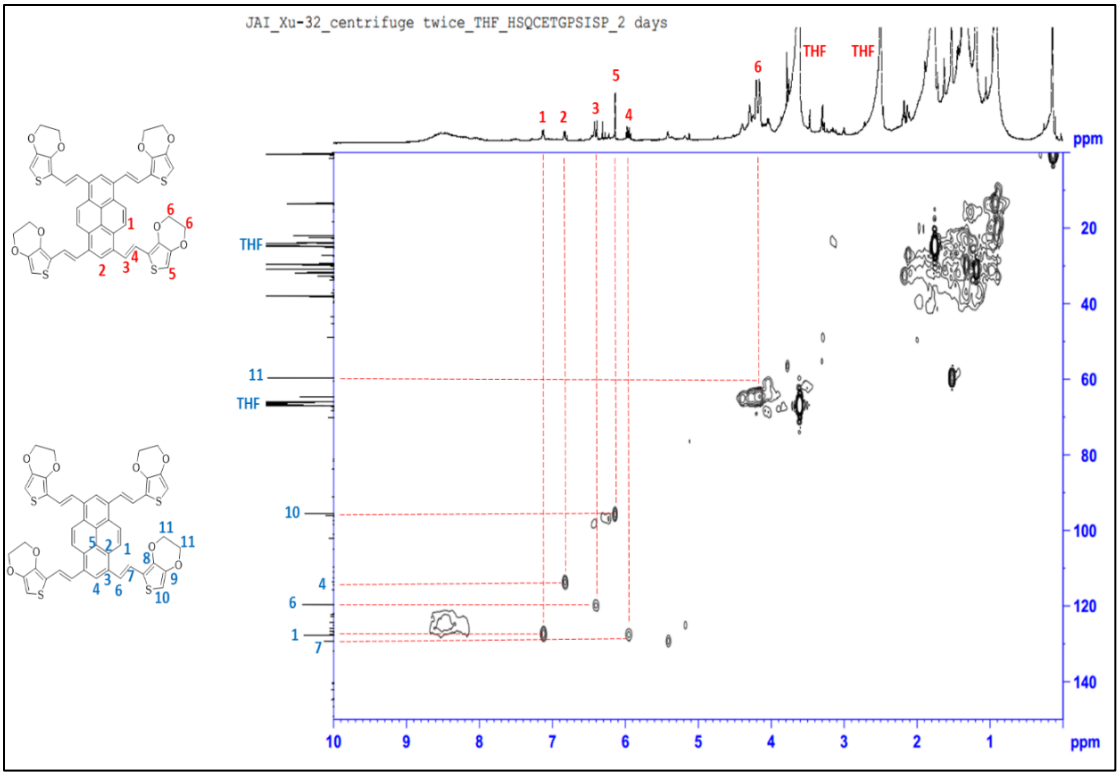

Figure 51. HSQC-NMR spectrum of P-(V-EDOT)$_4$

3.2 FTIR Spectra Analysis

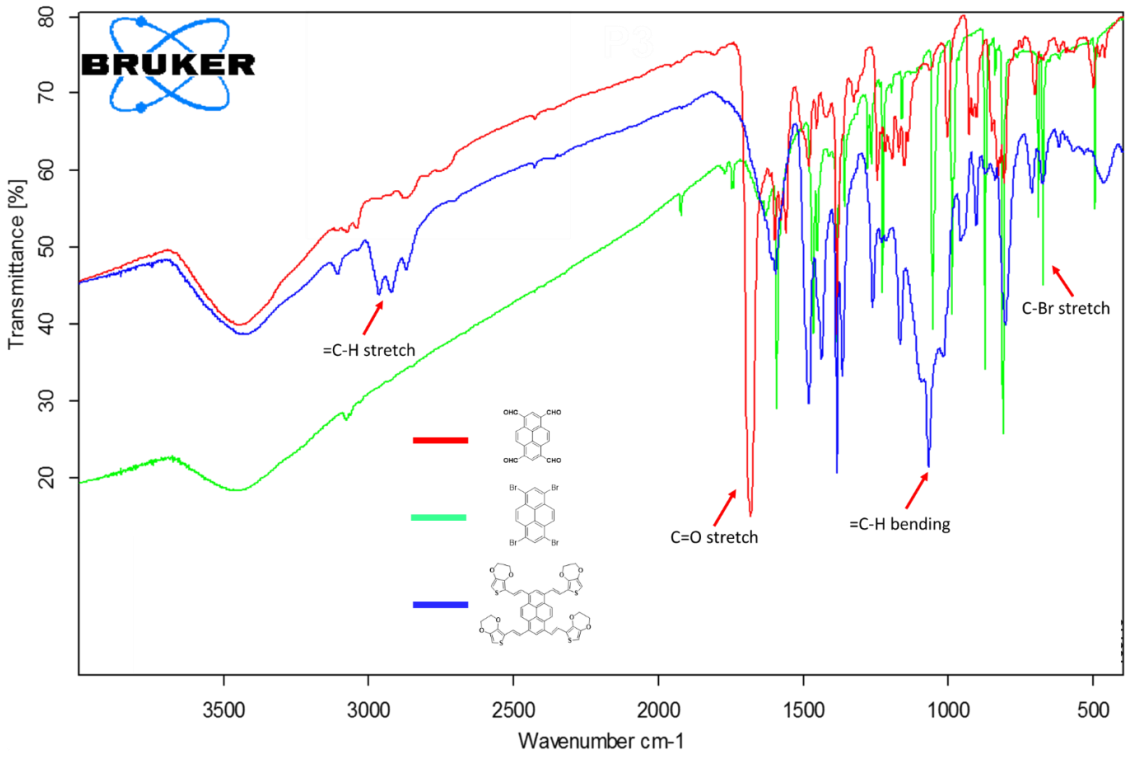

Figure 52. FTIR spectra comparisons P-Br_4 vs. P-A_4 vs. P-(V-EDOT)$_4$

The FTIR spectra in Fig. 49 show the formation and disappearance of the functional group peaks during the synthesis process towards the final P-(V-EDOT)$_4$ monomer. Due to the insolubility of P-Br_4, NMR spectroscopy cannot be used for its characterization. P-Br_4 has been synthesized previously [97] and the established FTIR spectrum is consistent with that obtained in this thesis.

In its FTIR spectrum (A.2), a strong narrow peak at 811 cm^{-1} was found corresponding to C-Br stretch, which completely disappeared in the FTIR spectrum of P-A_4 (A.4), in which a strong peak formed 1682 cm^{-1} corresponding to C=O stretch, indicating that the four C-Br bonds had been replaced by CHO groups. Interestingly, in the FTIR spectrum of P-(V-EDOT)$_4$ (A.10), the strong C=O stretch disappeared while a medium strong peak at 1596 cm^{-1} was found corresponding to C=C stretch; noticeably, a strong broad peak at 1067 cm^{-1} was found corresponding to =C-H bending with the existence of a broad peak at around 2921 cm^{-1} corresponding to =C-H stretch, indicating

that the four CHO groups at the edges of the pyrene backbone had been replaced with vinylene groups.

3.3 Conductivity Measurements

Conductivity Measurements were performed on PEDOT, poly-(P-(V-EDOT)$_4$) and poly-(P-(V-EDOT)$_4$ - co - EDOT) using a four-point collinear probe. However, this technique does not measure the conductivity (σ) directly; it can measure voltage (V) resulting from an applied current (I). Resistivity can be calculated using the equation: [103]

$$\rho = \frac{\pi}{ln2}\frac{V}{I}\,tk = 4.533\,\frac{V}{I}tk$$

where:

ρ = the resistivity (Ω·cm)

V = the voltage (V)

I = the magnitude of the source current (A)

t = the sample thickness (cm)

k = a correction factor (≈1)

The conductivity (σ) is the reciprocal of the Resistivity: $\sigma = \frac{1}{\rho}$ ($\Omega^{-1} \cdot cm^{-1}$ or S/cm).

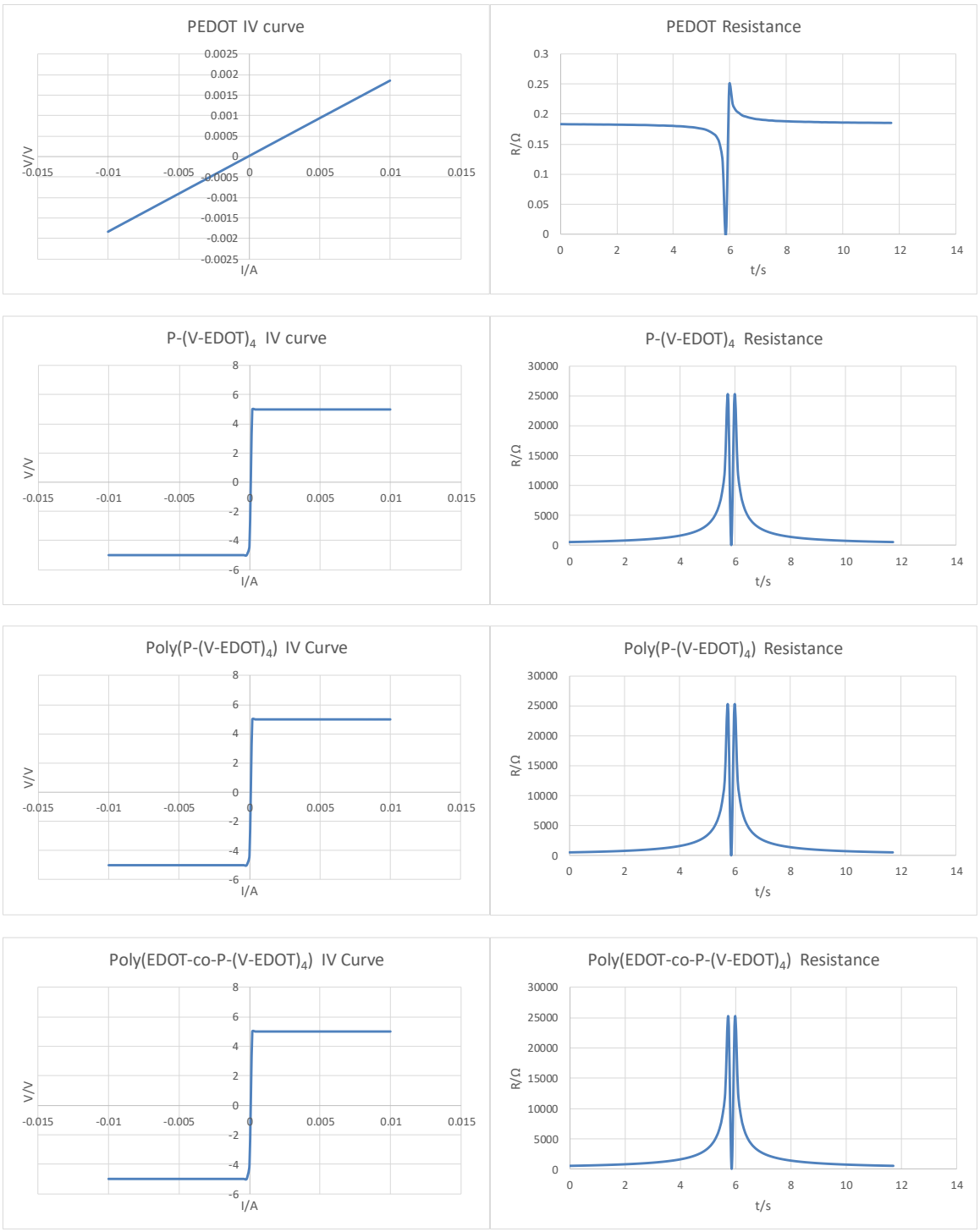

Figure 53. Current-Voltage (IV) curves and resistance curves measured using four-point probe

The IV curves tell the dynamic relationship between the voltage drop measured on the sample and the current applied on the sample. According to Ohm's law, the slope at a specific point of the IV curve expresses the resistance of the sample at that moment. The resistance of samples can be determined from the resistance curves, which tell the resistance of a sample as a function of applied current.

$$V = RI$$

Where:

V – Voltage (V)

R – Resistance (Ω)

I – Current (A)

For PEDOT, the IV curve shows a linear relation between voltage and current, which means the resistance of the PEDOT was invariant, which is about 0.18 Ω. Given the thickness of the sample (0.1250 cm), the conductivity is about 9.8 S/cm, which indicates that PEDOT prepared in this way is quite conductive and consistent with the conductivity of PEDOT: PSS reported previously, 10 S/cm, listed in Table 1.

Unfortunately, conductivity results obtained for the monomer P-(V-EDOT)$_4$ and polymers poly-(P-(V-EDOT)$_4$) and poly-(P-(V-EDOT)$_4$-co-EDOT), the curves are not desirable. Given that the current is sourced from -0.01A to 0.01A, in the IV curves of those polymers, the voltage went into compliance at 5V and -5V because the samples are very resistive, which produced a large voltage out of range of the source measure unit (5V). While a high conductivity was expected for the monomer, the high conductivity of the polymers was not. The high resistivity of these samples may be due to overoxidation to form disordered materials with poor electronic properties. The extended conjugation of these monomers may be the reason for this problem: while $FeCl_3$ is a common oxidant for typical electroactive monomers, it appears to be too strong for the monomer. More trials will focus on determining the proper choice of a milder oxidant for EDOT and P-(V-EDOT)$_4$ in the future work.

3.4 UV-VIS Spectra Analysis

As demonstrated in the UV-VIS spectra (Fig. 51), the absorbance peaks of pyrene found at 378nm, 356nm, 298nm, 281nm and 260nm correspond to a series of electronic transitions from π to π^* orbitals of the conjugated system, which is consistent with the literature spectrum.[104] For P-Br_4, absorptions are shifted to higher wavelengths (lower energy), indicating that tetrabromopyrene has a lower energy of transition state than that of pure pyrene. Absorptions at 425nm & 420nm (a doublet), 400nm, 317nm, 304nm, and 270nm result from the transitions from unshared bromine electrons to the antibonding σ^* and π^* orbitals of C-Br groups ($n \rightarrow \sigma^*$ and $n \rightarrow \pi^*$transitions) as well as excitation of aromatic π electrons to π^* antibonding orbitals ($\pi \rightarrow \pi^*$ transitions). For P-A_4, the energy of the transition state is further decreased; the absorptions are shifted to even lower energy at 460nm, 450nm, 428nm, and 330nm, due to $n \rightarrow \sigma^*$ and $n \rightarrow \pi^*$ transitions of C=O groups as well as excitation of aromatic π electrons to π^* antibonding orbitals ($\pi \rightarrow \pi^*$ transition).

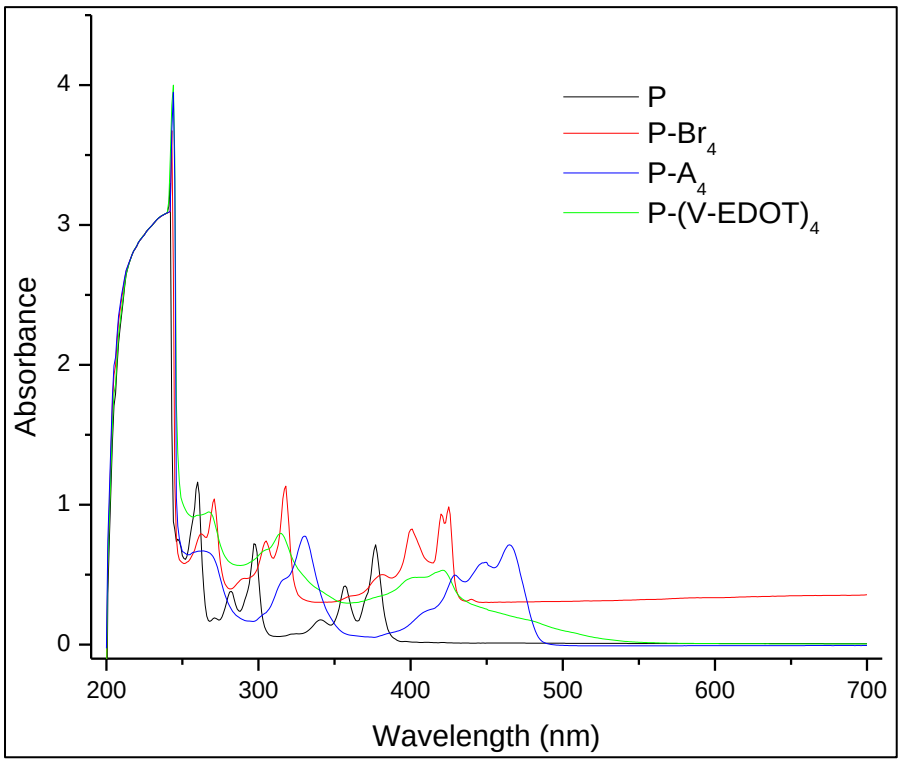

Figure 54. UV-VIS spectral comparison for pyrene (black), P-Br_4 (red), P- A_4 (blue) and P-$(V\text{-}EDOT)_4$ (green)

Interestingly, the absorbance peaks of the novel monomer P-(V-EDOT)$_4$ were found at 420nm, 400nm, and 315nm while literature reports [105] that the absorbance peak of PEDOT was found at 300nm – 450nm, indicating that the energy of the transition state of the monomer is lower than that of PEDOT, which also means that the oxidative potential of the monomer is lower than that of PEDOT. This phenomenon provides an evidence explaining the reason why $FeCl_3$, an oxidative reagent commonly used for chemical oxidative polymerization of EDOT, is not desirable for the monomer P-(V-EDOT)$_4$, causing overoxidation and high resistance of polymers. A milder oxidant is suggested for polymerization in the future work.

4. CONCLUSIONS AND FUTURE WORK

4.1 Conclusions

In this thesis, a tetrafunctionalized pyrene complex P-(V-EDOT)$_4$ has been designed and synthesized, which couples EDOT with a pyrene ring backbone via vinylene groups to form a highly-conjugated monomer. It has been characterized using NMR and FTIR, which confirm the conjugated linkage between pyrene ring and EDOT.

The monomer has been polymerized via chemical oxidative polymerization by itself and with additional EDOT to form poly-(P-(V-EDOT)$_4$) and poly-(P-(V-EDOT)$_4$ - co - EDOT), respectively. The conductivities of those polymers were determined via four-point probe measurements using PEDOT as the control. The result shows that the conductivity of PEDOT is 9.8 S/cm, while the conductivities of the other polymers are not desirable due to their large resistance that may have resulted from overoxidation during polymerization process.

UV-VIS spectra show that the energy of the transition state of the monomer P-(V-EDOT)$_4$ is lower than that of PEDOT, meaning that the oxidative potential of the monomer is lower than that of PEDOT.

4.2 Future Work

Chemical oxidative polymerization of P-(V-EDOT)$_4$ will be conducted with great caution on the purity of the monomer, and with emphasis on searching for a milder oxidant. Conductivity measurements will be performed on the desirable samples seeking for enhanced conductivity compared to PEDOT. Polymers will also be prepared using electrochemical polymerization. Functionalized graphene derivatives will be prepared via the same techniques routine used for P-(V-EDOT)$_4$, from which ICPs with graphene cores will be synthesized.

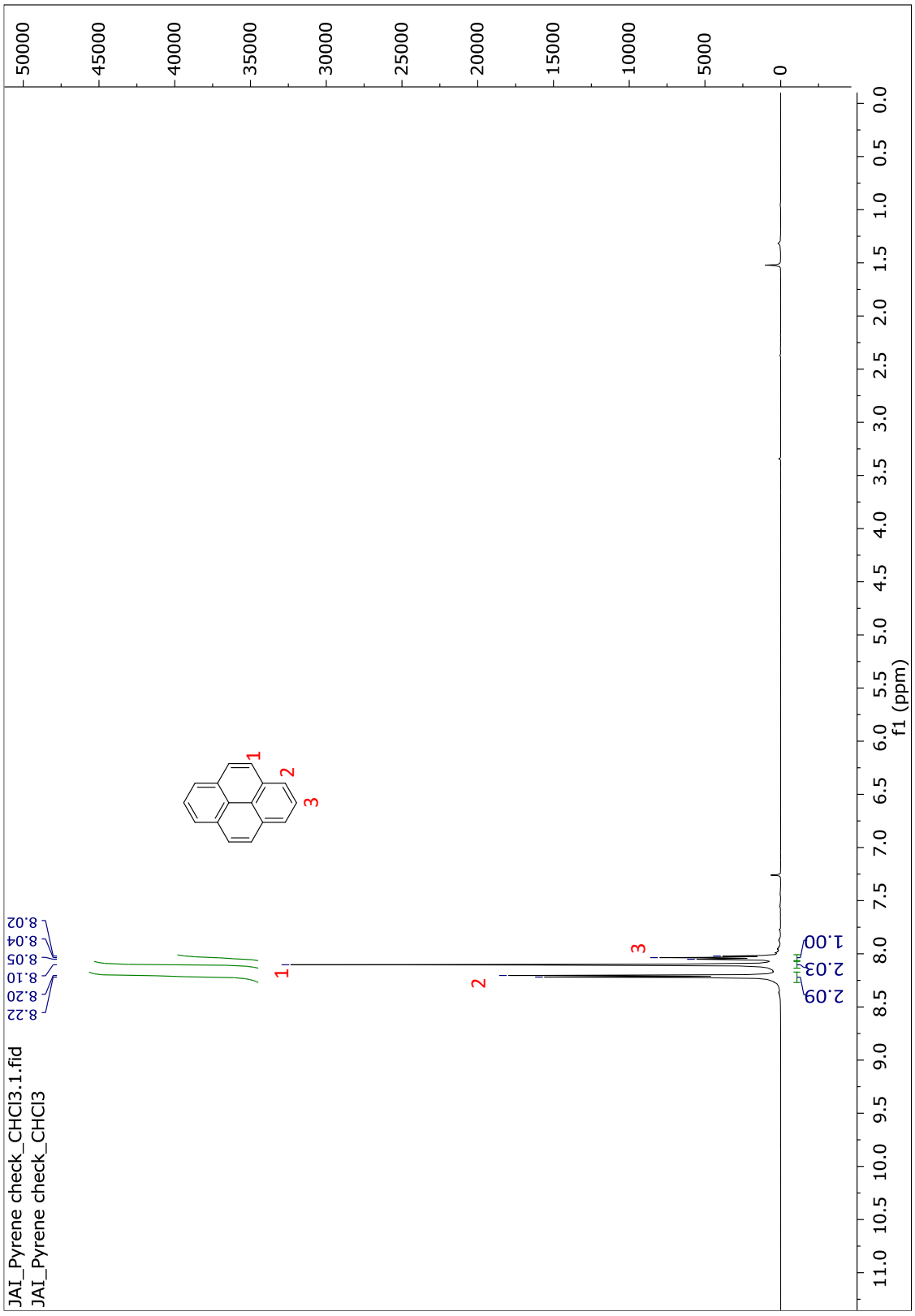

A.1 ^{1}H NMR spectrum of pyrene

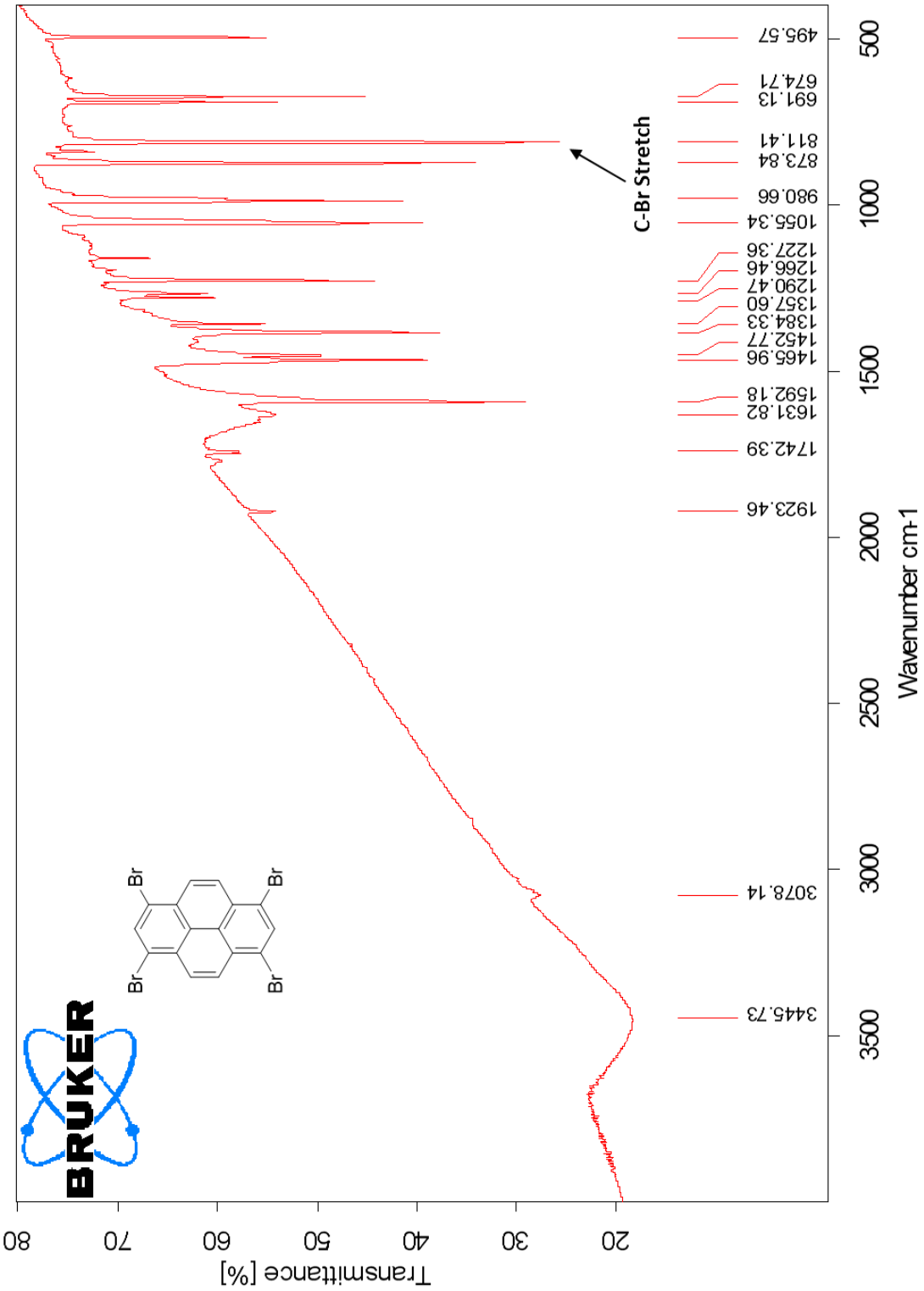

A.2 FTIR spectrum of 1,3,6,8-tetrabromopyrene

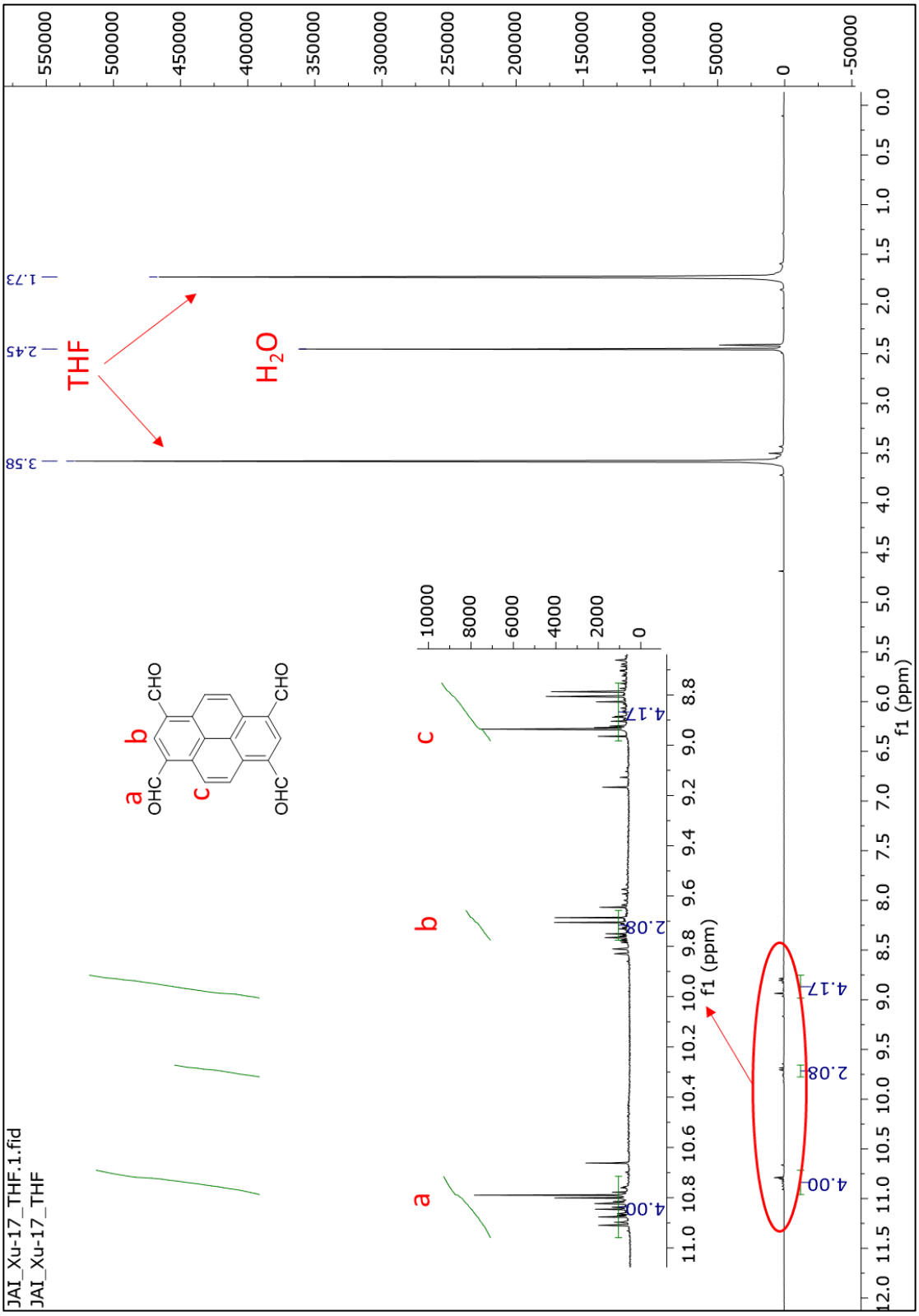

A.3 ^{1}H NMR spectrum of 1,3,6,8-pyrene tetracarbaldehyde

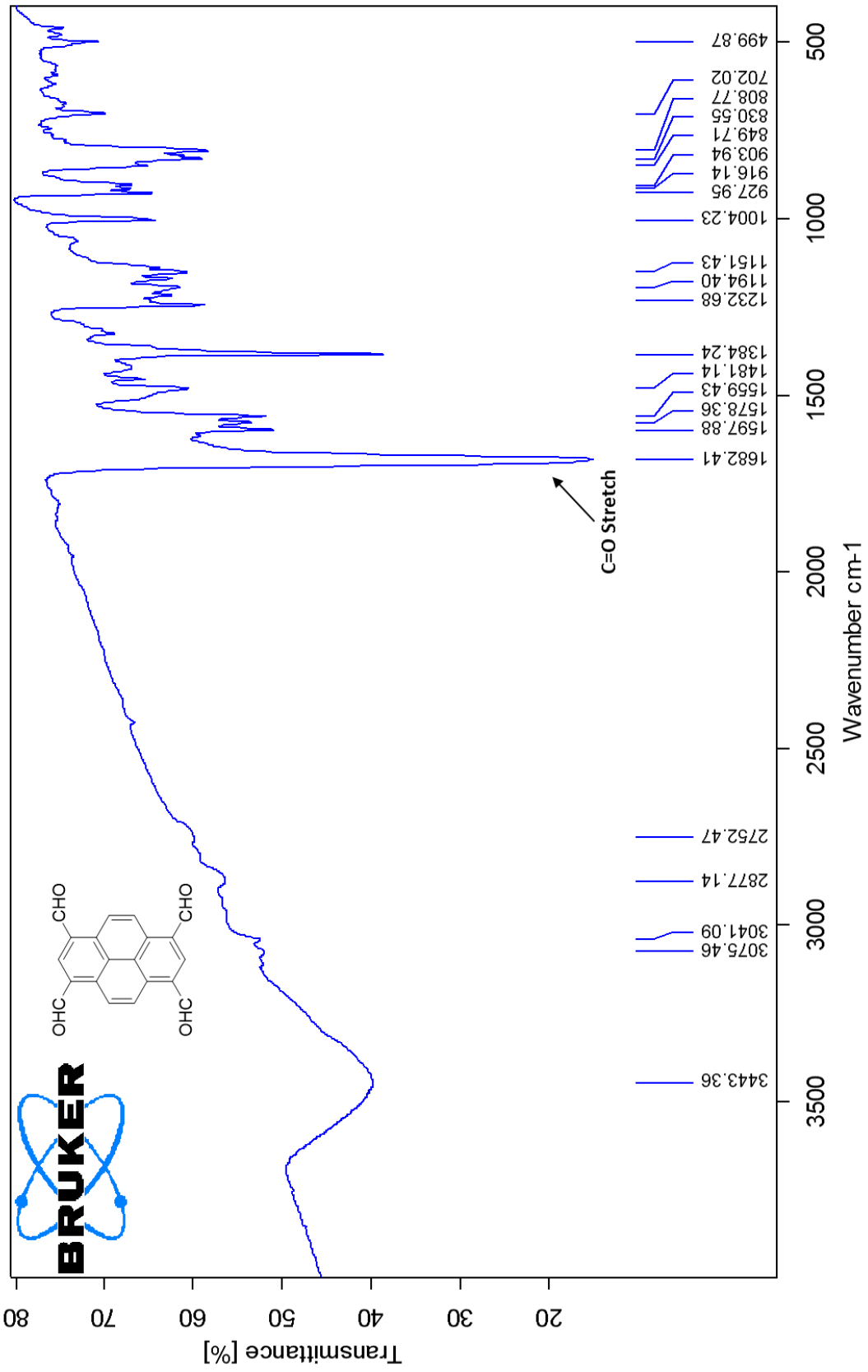

A.4 FTIR spectrum of 1,3,6,8-pyrene tetracarbaldehyde

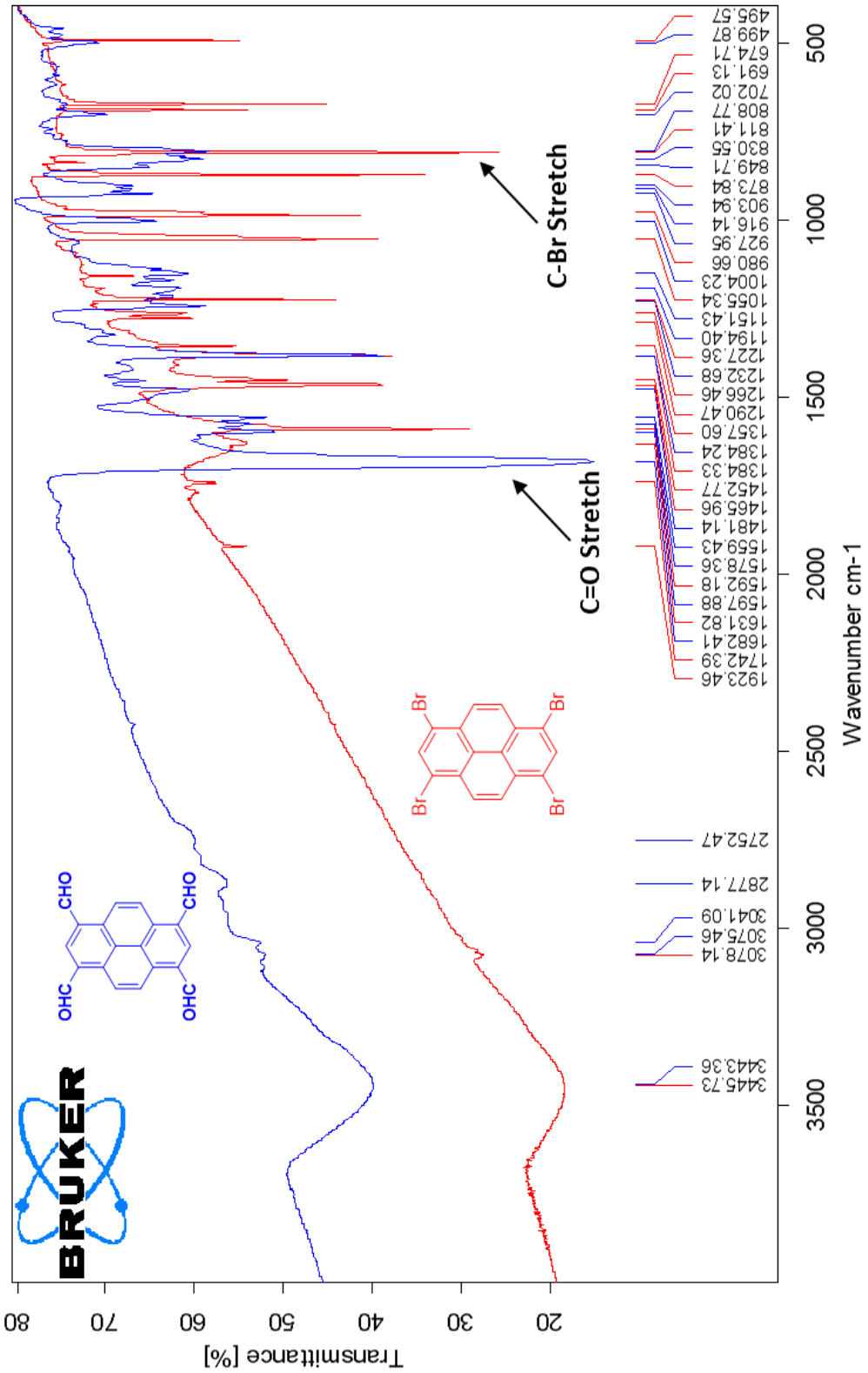

A.5 Spectral comparison of 1,3,6,8-pyrene tetracarbaldehyde vs. 1,3,6,8-tetrabromopyrene

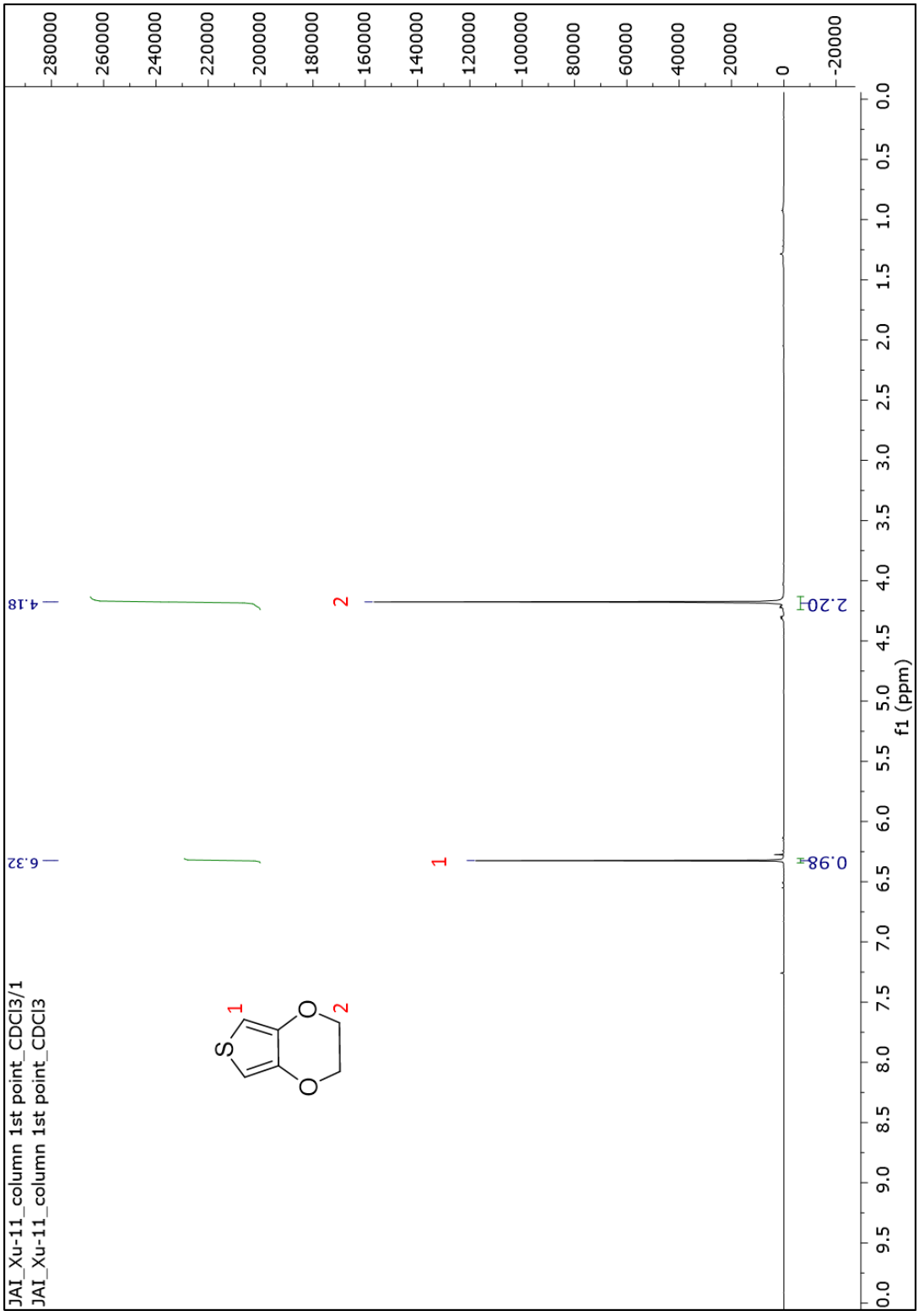

A.6 ^{1}H NMR spectrum of EDOT

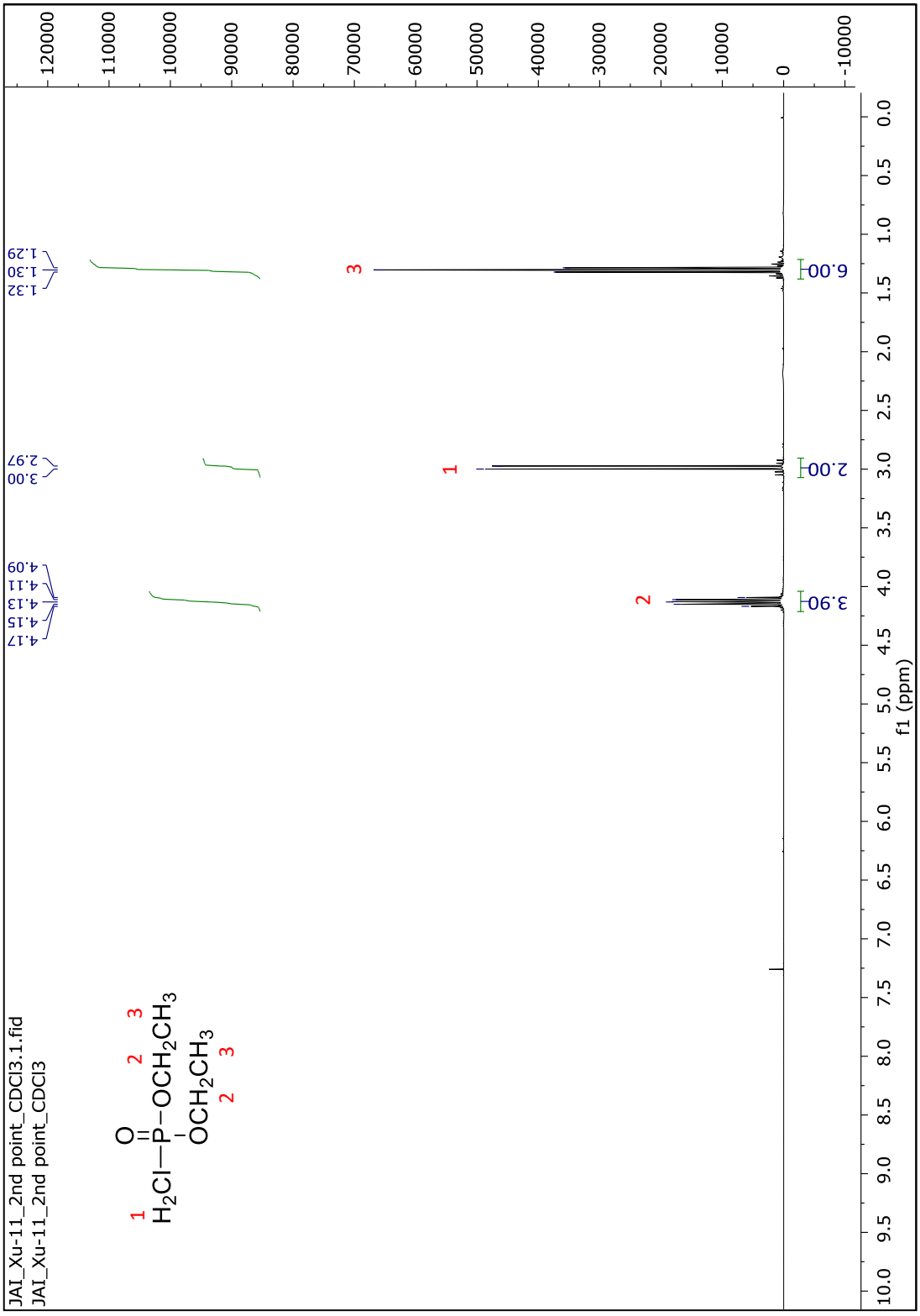

A.7 ^{1}H NMR spectrum of diethyl-iodomethylphosphonate

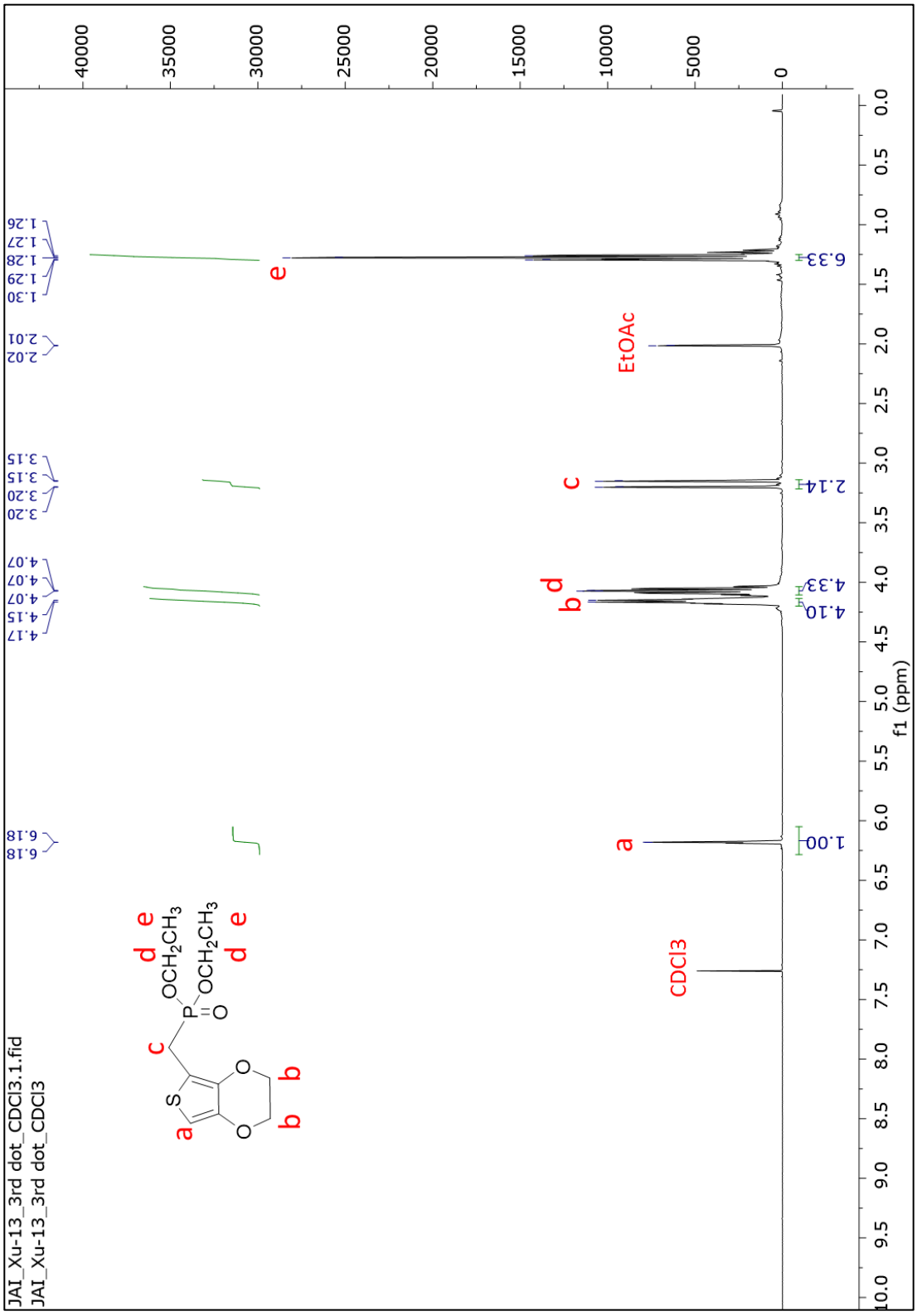

A.8 ^{1}H NMR spectrum of EDOT-PE

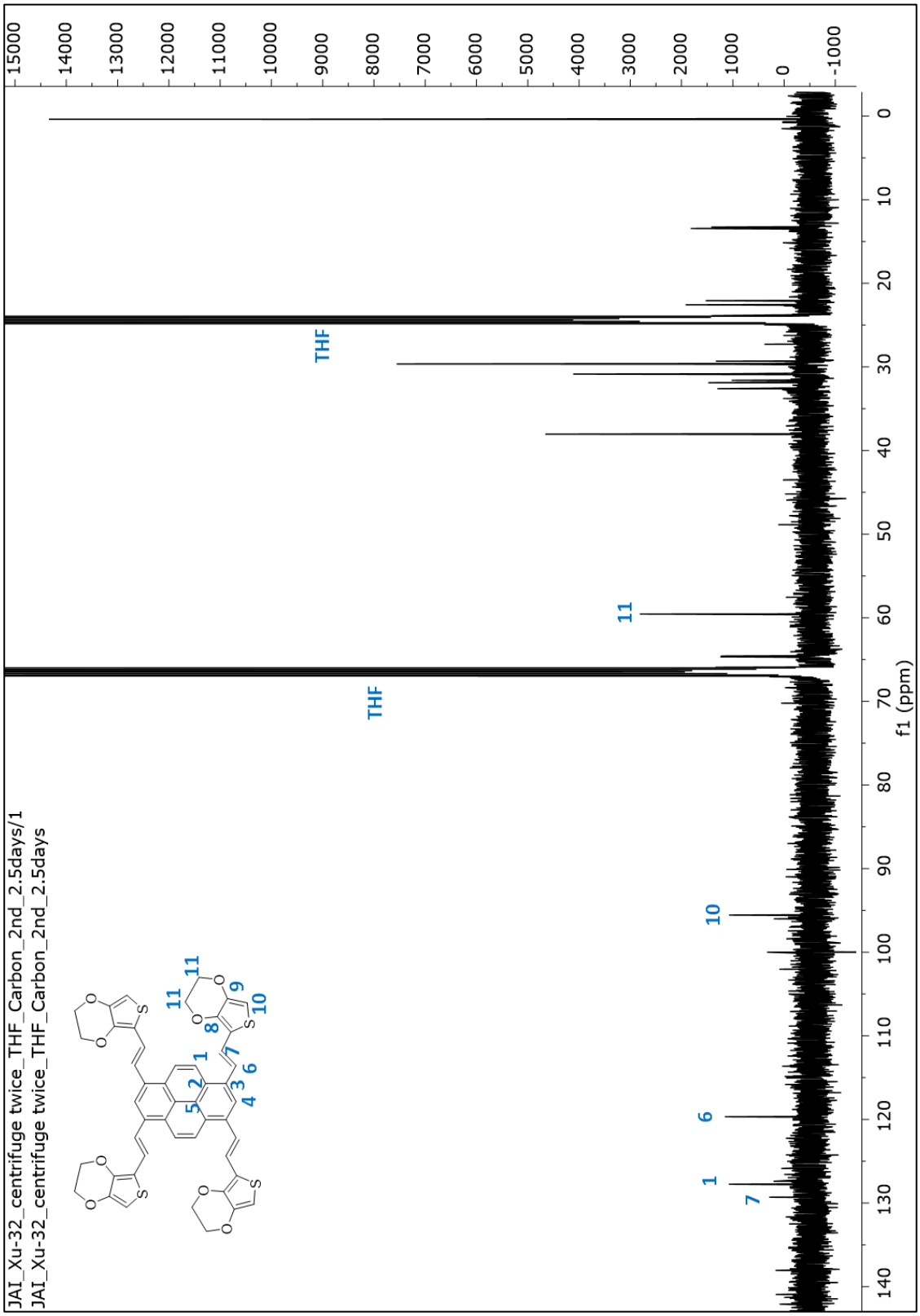

A.9 ^{13}C NMR spectrum of P-(V-EDOT)$_4$

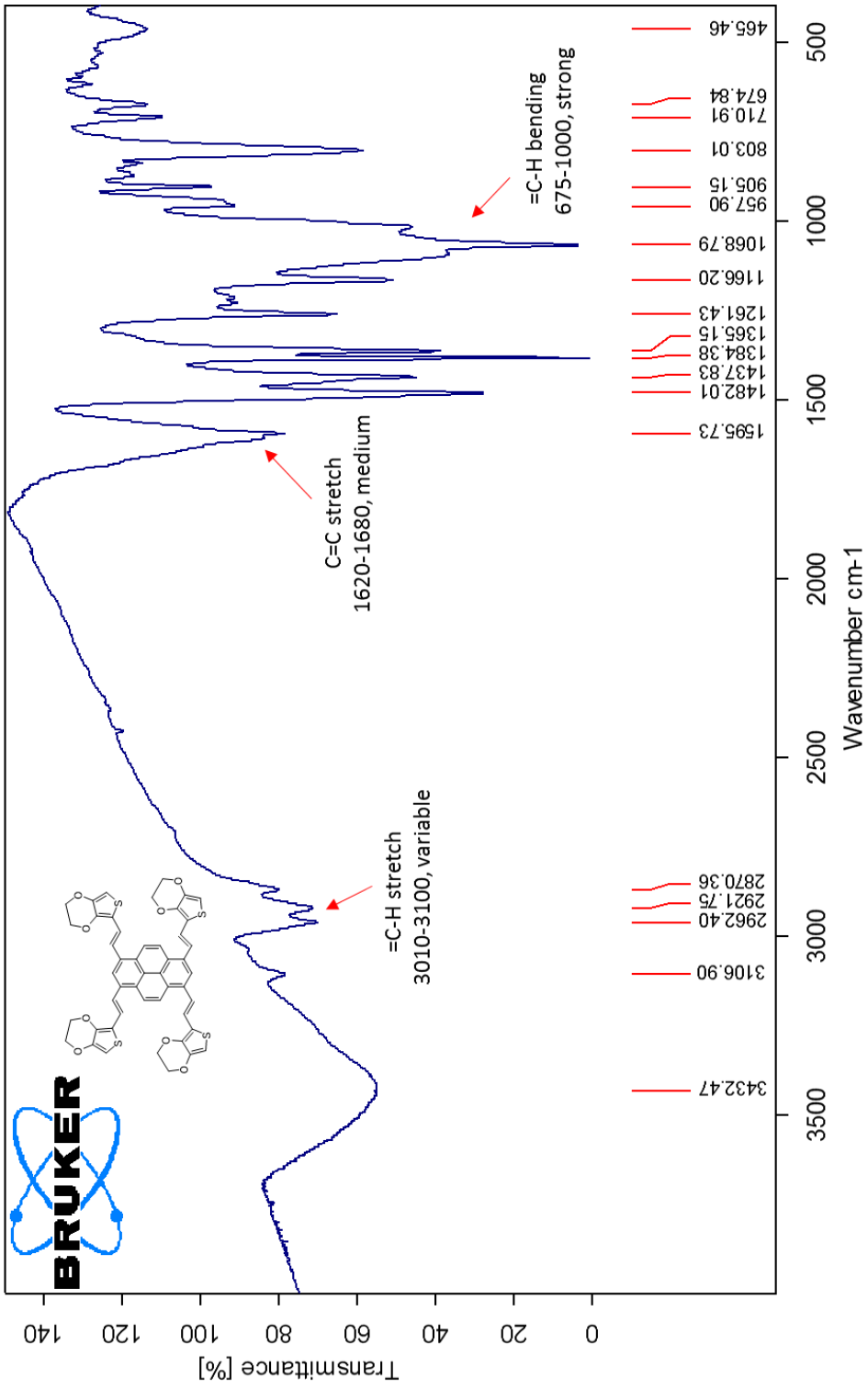

A.10 FTIR spectrum of P-(V-EDOT)$_4$

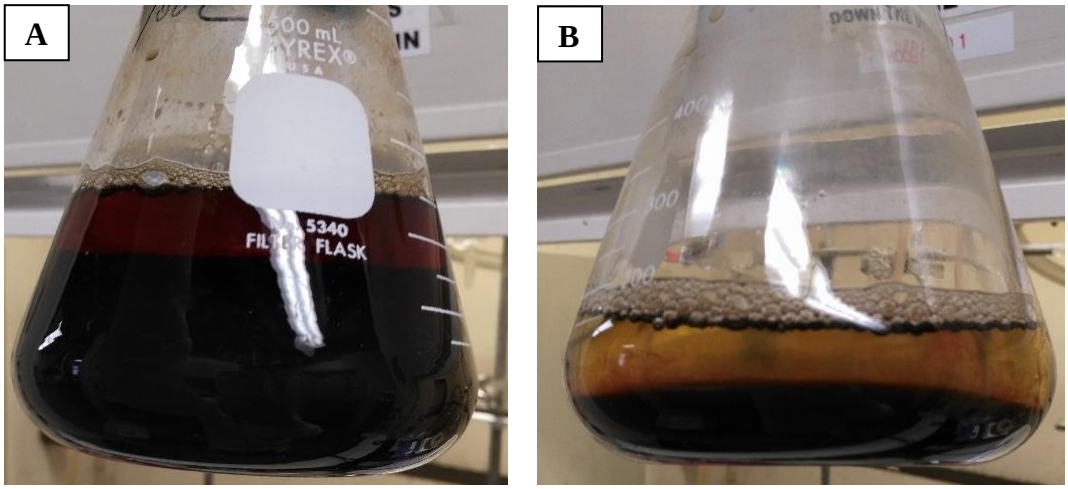

HA in base solution (pH = 10) HA in acid solution (pH = 2)

A.11 Humic acid (HA) suspension in solution

REFERENCES

1. Ateh, DD; Navsaria, HA; Vadgama, P. Polypyrrole-based conducting polymers and interactions with biological tissues. *J. R. Soc. Interface* **2006**, *3*, 741–752.
2. Murat, Ates. A review study of (bio)sensor systems based on conducting polymers. *Mater. Scie. Engin. C* ***2013***, *33*, 1853–1859.
3. Zarras, P.; In *Encyclopedia of Polymer Science and Technology, Concise 3rd ed.*; Wiley Interscience: New York, **2004**, 351–358.
4. Irvin, J. A.; Carberry, J. R. Dominant Ion Transport Processes of Ionic Liquid Electrolyte in Poly(3,4-ethylenedioxythiophene). *J. Poly. Sci., Part B: Polymer Physics*, **2013**, *51*, 337–342.
5. Shirakawa, H.; Louis, E. J.; MacDiarmid, A. G.; Chiang, C. K.; Heeger, A. J. Synthesis of electrically conducting organic polymers: halogen derivatives of polyacetylene, (CH)x. *J. Chem. Soc. Chem. Commun.* **1977**, 578–580.
6. Zhou, D. D.; Cui, X. T.; Hines, A; Greenberg, R. J. *Conducting polymers in neural stimulation applications*. Springer: Berlin, **2010**.
7. Guimard, N. K.; Gomez, N.; Schmidt, C. E. Conducting polymers in biomedical engineering. *Prog. Polym. Sci.* **2007**, *32*, 876–921.
8. Deepa, M., Ahmad, S. Polypyrrole films electropolymerized from ionic liquids and in a traditional liquid electrolyte: A comparison of morphology and electro–optical properties. *Eur. Polym. J.* **2008**, *44*, 3288–3299.
9. Han, D.H., H.J.; Lee, S.M.; Park, S. M. Electrochemistry of conductive polymers XXXV: Electrical and morphological characteristics of polypyrrole films prepared in aqueous media studied by current sensing atomic force microscopy. *Electrochim. Acta*, **2005**, *50*, 3085–3092.
10. Garner, B.; Georgevich, A; Hodgson, A. J.; Liu, L.; Wallace, G.G. Polypyrrole–heparin composites as stimulus-responsive substrates for endothelial cell growth. *J. Biomed. Mater. Res.* **1999**, *44*, 121–129.
11. Garner, B.; Hodgson, A.J.; Wallace, G. G.; Underwood, P. A. Human endothelial cell attachment to and growth on polypyrrole-heparin is fibronectin dependent. *J. Mater. Sci. Mater. Med.* **1999**, *10*, 19–27.

12. Ferraz, N.; Stromme, M.; Fellstrom, B.; Pradhan, S.; Nyholm, L.; Mihranyan A. In vitro and in vivo toxicity of rinsed and aged nanocellulose–polypyrrole composites. *J. Biomed. Mater. Res.* A **2012**, *100a*, 2128–38.
13. Kumar, D.; Sharma, R. C. Advances in conductive polymers. *Eur. Polym. J.* **1998**, *34*, 1053-1060.
14. Wan M. In *Introduction of conducting polymers-Conducting polymers with micro or nanometer structure*. Springer: Berlin, **2008**.
15. Ribo, J.M.; Acero, C.; Anglada, M.C.; Dicko, A.; Tura, J.M.; Ferrer-Anglada N.; Albareda, A. On the structure and transport properties of polypyrroles. *Butll. Soc. Cat. Cien.* **1992,** *Vol. XIII, Num.1,* 335-351.
16. Chronakis, I. S.; Grapenson, S; Jakob, A. Conductive polypyrrole nanofibers via electrospinning: electrical and morphological properties. *Polymer*. **2006**, *47*, 1597–1603.
17. Bousalem, S.; Yassar, A.; Basinska, T.; Miksa, B.; Slomkowski, S.; Azioune, A.; Chehimi, M. M. Synthesis, characterization and biomedical applications of functionalized polypyrrole-coated polystyrene latex particles. *Polym. Adv. Technol.* **2003**, *14*, 820-825.
18. Li, Y; Neoh, K. G.; Kang, E. T. Plasma protein adsorption and thrombus formation on surface functionalized polypyrrole with and without electrical stimulation. *J. Colloid Interf. Sci.* **2004**, *275*, 488–95.
19. Cui, X.; Hetke, J. E.; Wiler, J. A.; Anderson, D. J.; Martin, D.C. Electrochemical deposition and characterization of conducting polymer polypyrole/PSS on multichannel neural probes. *Sens. Actuator A-Phys.* **2001**, *93*, 8–18.
20. Ramanaviciene, A.; Malinauskas, A; Malinauskas, A. Electrochemical sensors based on conducting polymer—polypyrrole. Visualization of red-ox proteins on the gold surface using enzymatic polypyrrole formation. *Electrochim. Acta.* **2006**, *51*, 6025–6037.
21. Li, H.; Zhou, Q.; Audebert, P.; Miomondre, F.; Allain, C.; Yang, F.; Tang, J. New conducting polymers functionalized with redox-active tetrazines *J. Electroanal. Chem.* **2012**, *668*, 26–29.

22. Chen, W.; Lei, Y.; Li, C.M. Regenerable Leptin Immunosensor Based on Protein G Immobilized Au-Pyrrole Propylic Acid-Polypyrrole Nanocomposite. *Electroanalysis.* **2010**, *22 (10)*, 1078–1083.
23. Ramanaviciene, A.; Kausaite-Minkstimiene, A.; Oztekin, Y.; Carac, G.; Voronovic, J.; German, N.; Ramanavicius, A. Visualization of red-ox proteins on the gold surface using enzymatic polypyrrole formation. *Microchimica Acta.* **2011**, *10*, 175-179.
24. Meng, S.; Rouabhia, M.; Shi, G.; Zhang, Z.; Heparin dopant increases the electrical stability, cell adhesion, and growth of conducting polypyrrole/poly(L,Llactide) composites. *J. Biomed. Mater. Res.* **2008**, *87A*, 332–344.
25. Brahim; S., Guiseppi-Elie. A.; Electroconductive hydrogels: electrical and electrochemical properties of polypyrrole–poly(HEMA) composites. *Electroanalysis.* **2005**, *17*, 556-70.
26. Lee, J.W.; Serna, F.; Nickels, J.; Schmidt, C.E. Carboxylic acid-functionalized conductive polypyrrole as a bioactive platform for cell adhesion. *Biomacromolecules* **2006**, *7*, 1692–1695.
27. Tokonami, S.; Saimatsu, K.; Nakadoi, Y.; Furuta, M.; Shiigi, H.; Nagaoka, T. Vertical Immobilization of Viable Bacilliform Bacteria into Polypyrrole Films *Anal. Sci.* **2012**, *28 (4)*, 319–321.
28. Zhang, A.J.; Chen, J.; Niu, D. F.; Wallace, G. G.; Lu, J. X. Electrochemical polymerization of pyrrole in BMIMPF6 ionic liquid and its electrochemical response to dopamine in the presence of ascorbic acid. *Synth. Met.* **2009**, *159 (15–16)*, 1542–1545.
29. Berdichevsky, Y.; Lo, Y. H. Polypyrrole Nanowire Actuators. *Adv. Mater.* **2006**, *18*, 122–125.
30. Liu, Q.; Wang, Y.; Zhang, Y. J.; Xu, S.C.; Wang, J.X.; Effect of dopants on the adsorbing performance of polypyrrole/graphite electrodes for capacitive deionization process. *Synth. Met.* **2012**, *162 (7-8)*, 655–661.
31. Ghasemi-Mobarakeh, L.; Prabhakaran, M. P.; Morshed, M.; Nasr-Esfahani, M. H.; Baharvand, H.; Kiani, S.;Al-Deyab, S. S. Application of conductive polymers, scaffolds and electrical stimulation for nerve tissue engineering. *J. Tissue Eng. Regen. Med.* **2011**, *5*, 17–35.

32. Epstein, A. J. *Electrical conductivity in conjugated polymers-Conductive polymers and plastics in industrial applications.* Norwich, NY: William Andrew Publishing/Plastics Design Library; **1999**, 1–9.
33. MacDiarmid, A.G.; Epstein, A.J. Secondary doping in polyaniline. *Synth. Met.*, **1995**, *69*, 85–92.
34. MacDiarmid, A. G.; Chiang, J. C.; Richter, A. F. Polyaniline: a new concept in conducting polymers. *Synth. Met.*, **1987**, *18*, 285–290.
35. Pouget, J. P.; Jdzefowiczt, M. E.; Epstein, A. J.; Tang, X.; MacDiarmid, A.G. X-ray structure of polyaniline. *Macromolecules*, **1991**, *24*, 779–789.
36. Tourillon, G.; Garnier, F. Morphology and crystallographic, structure of polythiophene and derivatives. *Mol. Cryst. Liq. Cryst.* **1985**, *118*, 221–226.
37. Cullen, D.K.; Patel, A.R.; Doorish, J.F.; Smith, D.H.; Pfister, B.J. Developing a tissueengineered neural-electrical relay using encapsulated neuronal constructs on conducting polymer fibers. *J. Neural. Eng.* **2008**, *5*, 374–384.
38. Borriello, A.; Guarino, V.; Schiavo, L.; Alvarez-Perez, M. A.; Ambrosio, L. Optimizing PANi doped electroactive substrates as patches for the regeneration of cardiac muscle. *J. Mater. Sci. Mater. Med.* **2011**, *22*, 1053–62.
39. Guo, Y.; Mylonakis, A.; Han, J.; MacDiarmid, A. G.; Chen, X.; Lelkes, P. I.; Wei, Y. Electroactive oligoaniline-containing self-assembled monolayers for tissue engineering applications. *Biomacromolecules*, **2007**, *8*, 3025–3034.
40. Prabhakaran, M. P.; Ghasemi-Mobarakeh, L.; Jin, G.; Ramakrishna, S. Electrospun conducting polymer nanofibers and electrical stimulation of nerve stem cells. *J. Biosci. Bioeng.*, **2011**, *112*, 501–507.
41. Yu, Q. Z.; Shi, M. M; Deng, M.; Wang, M.; Chen, H. Z. Morphology and conductivity of polyaniline sub-micron fibers prepared by electrospinning. *Mater. Sci. Eng. B Solid*, **2008**, *150*, 70–76.
42. Heinze, J.; Frontana-Uribe, B. A.; Ludwigs, S.; Electrochemistry of conducting polymerss - persistent models and new concepts. *Chem. Rev.* **2010**, *110*, 4724 – 4771.
43. Huynh, T. P.; Sharma, P. S.; Sosnowska, M.; D'Souza, F; Kutner, W. Functionalized polythiophenes: Recognition materials for chemosensors and biosensors of superior sensitivity, selectivity, and detectability. *Prog. Poly Sci*. 2015, *47*, 1–25.

44. Jonas, F.; Heywang, G.; Werner, S. Novel polythiophenes, process for their preparation, and their use. DE 3813589, 22 April **1988**.
45. Aasmundtveit, K.E.; Samuelsent, E.J.; Pettersson, L. A.; Inganas, O.; Johansson, T.; Feidenhans, R. Structure of thin films of poly(3,4-ethylenedioxythiophene. *Synth. Met.* **1999**, *101*, 561-564.
46. Peramo, A.; Urbanchek, M.G.; Spanninga, S.A.; Povlich, L.K.; Cederna, P.; Martin, D.C. In situ polymerization of a conductive polymer in acellular muscle tissue constructs. *Tissue Eng. Part A* **2008**, *14*, 423–432.
47. Thomas, C. A.; Zong, K.; Schottland, P.; Reynolds, J. R. Poly(3,4-alkylenedioxypyrrole)s as highly stable aqueous-compatible conducting polymers with biomedical implications. *Adv. Mater.* **2000**, *12*, 222–225.
48. Po, R.; Carbonera, C.; Bernardi, A.; Tinti, F.; Camaioni, N. *Sol. Energy, Mater. Sol. Cells*. **2012**, *100*, 97–114.
49. Sun, K.; Zhang, S.; Li, P.; Xia, Y.k Zhang, X.; Du, D.; Isikgor, F. H.; Ouyang, J. Review on application of PEDOTs and PEDOT: PSS in energy conversion and storage devices. *J. Mater. Sci.: Mater Electron*. **2015**, *26*, 4438-4462.
50. Kim, J.Y.; Kwon, M.H.; Min, Y.K.; Kwon, S.; Ihm, D.W. Self-assembly and crystalline growth of poly(3,4-ethylenedioxythiophene) nanofilms. *Adv. Mater.* **2007**, *19*, 3501–3506.
51. Cho, B.; Park, K.S.; Baek, J.; Oh, H.S.; Koo Lee, Y.-E.; Sung, M.M. Single-crystal poly(3,4-ethylenedioxythiophene) nanowires with ultrahigh conductivity. *Nano Lett.* **2014**, *14*, 3321–3327.
52. Massonnet, N.; Carella, A.; de Geyer, A.; Faure-Vincent, J.; Simonato, J.-P. Metallic behaviour of acid doped highly conductive polymers. *Chem. Sci.* **2015**, *6*, 412–417.
53. Ummartyotin, S.; Juntaro, J.; Wu, C.; Sain, M.; Manuspiya, H. Deposition of PEDOT: PSS nanoparticles as a conductive microlayer anode in OLEDs device by desktop inkjet printer. *J. Nanomater*. **2011**, Article ID 606714.
54. Elschner, A.; Kirchmeyer, S.; Lövenich, W.; Merker, U.; Reuter, K. *PEDOT: Principles and Applications of an Intrinsically Conductive Polymer*. CRC Press: Boca Raton, FL, USA, **2010**.

55. Roth, S.; Carroll, D. One-dimensional metals – conjugated polymers, organic crystals, carbon nanotubes. 2nd ed. *WILEY-VCH Verlag GmbH & Co. KGaA, Weinheim*. **2004.**
56. Su, W. P.; Schrieffer, J. R. Soliton dynamics in polyacetylene. *Proc. Natl. Acad. Sci. USA.* **1980**, *77*, 5626.
57. Kaynak, A.; Rintoul, L.; George, G. A. Change of mechanical and electrical properties of polypyrrole films with dopant concentration and oxidative aging. *Mater. Res. Bull.* **2000**, *35*, 813–824.
58. Liu, X.; Gilmore, K. J.; Moulton, S. E.; Wallace, G. G. Electrical stimulation promotes nerve cell differentiation on polypyrrole/poly(2-methoxy-5 aniline sulfonic acid) composites. *J. Neural. Eng.* **2009**, *6*, 1–10.
59. Shi, G.; Rouabhia, M.; Wang, Z.; Dao, L. H.; Zhang, Z. A novel electrically conductive and biodegradable composite made of polypyrrole nanoparticles and polylactide. *Biomaterials*, **2004**, *25*, 2477–2488.
60. Kumara, D.; Sharmaa, R. C. Advances in conductive polymers. *Eur. Polym. J.*, **1998**, Vol. 34, Issue 8, 1053-1060.
61. Brown, W. H.; Iverson, B. L.; Anslyn, E. V.; Foote, C. S. Organic Chemistry, 7th ed. WANSWORTH.
62. Ravichandran, R.; Sundarrajan, S.; Venugopal, J. R.; Mukherjee, S.; Ramakrishna, S. Applications of conducting polymers and their issues in biomedical engineering. *J. R. Soc. Interface*, **2010**, *7*, 559–579.
63. Balint, R.; Cassidy, N. J.; Cartmell, S. H. Conductive polymers: Towards a smart biomaterial for tissue engineering. *Acta Biomaterialia*. 2014, 10, 2341–2353.
64. Tan, Y; Ghandi, K. Kinetics and mechanism of pyrrole chemical polymerization. *Synth. Met.* **2013**, *175*, 183–191.
65. Armes, S. P. Optimum reaction conditions for the polymerization of pyrrole by iron (III) chloride in aqueous solution. *Synth. Met.* **1987**, *20*, 365–71.
66. Calvo, P. A; Rodriguez, J.; Grande, H.; Mecerreyes, D.; Pomposo, J. A. Chemical oxidative polymerization of pyrrole in the presence of m-hydroxybenzoic acid- and m-hydroxycinnamic acid-related compounds. *Synth Met.* **2002**, *126*, 111–116.

67. Martins, N. C. T.; Silva, M. T.; Montemora, M. F.; Fernandes, J. C. S.; Ferreira, M. G. S. Electrodeposition and characterization of polypyrrole films on aluminium alloy 6061-T6. *Electrochim Acta*, **2008**, *53*, 4754–4763.
68. Herrasti, P.; Diaz, L.; Ocin, P.; Lbanez, A.; Fatas, E. Electrochemical and mechanical properties of polypyrrole coatings on steel. *Electrochim Acta*, **2004**, *49*, 3693-3699.
69. Choi, S.; Park, S. Electrochemistry of conductive polymers. XXVI. Effects of electrolytes and growth methods on polyaniline morphology. *J. Electrochem. Soc.* **2002**, *149*, 26-34.
70. Li, C. M.; Sun, C. Q.; Chen, W.; Pan, L. Electrochemical thin film deposition of polypyrrole on different substrates. *Surf. Coat Technol.* **2005**, *198*, 474-477.
71. Wallace, G. G.; Smyth, M.; Zhao, H. Conducting electroactive polymer-based biosensors. *Trends Analyt. Chem.*, **1999**, *18*, 245-251.
72. Patra, S.; Barai, K.; Munichandraiah, N. Scanning electron microscopy studies of PEDOT prepared by various electrochemical routes. *Synth. Met.*, **2008**, *158*, 430–435.
73. Mondal, S. K.; Prasad, K. R.; Munichandraiah, N. Analysis of electrochemical impedance of polyaniline films prepared by galvanostatic, potentiostatic and potentiodynamic methods. *Synth. Met.*, **2005**, *148*, 275–286.
74. Allen, M.J.; Tung, V. C.; Kaner, R. B. Honeycomb Carbon: A Review of Graphene, *Chem. Rev.* **2010**, *110*, 132–145.
75. Stolyarova, E; Rim, K. T.; Ryu, S.; Maultzsch, J.; Kim, P.; Brus, L. E.; Heinz, T. F.; Hybertsen, M. S.; Flynn G. W. High-resolution scanning tunneling microscopy imaging of mesoscopic graphene sheets on an insulating surface. *Proc. Natl. Acad. Sci. U.S.A.* **2007**, *104*, 9209.
76. Georgakilas, V.; Otyepka, M.; Bourlinos, A. B.; Chandra, V.; Kim, N.; Kemp, K. C.; Hobza, P.; Zboril, R.; Kim, K. S. Functionalization of Graphene: Covalent and Non-Covalent Approaches, Derivatives and Applications. *Chem. Rev.* **2012**, 112.
77. D. Li, M.B. Muller, S. Gijle, R.B. Kaner, G.G. Wallace. Processable aqueous dispersions of graphene nanosheets. *Nat Nanotechnol*. 2008, *3*, 101–105.
78. Hummers, W. S., Jr.; Offeman, R.E. Preparation of Graphitic Oxide. *J. Am. Chem. Soc*. **1958**, *80*, 1339.

79. Nasrollahzadeh, M.; Banaei, F.; Fakhri, P.; Jaleh, B. Synthesis, characterization, structural, optical properties and catalytic activity of reduced graphene oxide/copper nanocomposites, *RSC Adv.*, **2015**, *5*, 10782-10789.
80. Beall, G. Method and System for Producing Graphene and Graphenol, U.S. Patent Application 2011/0201739 A1, Aug. 18, **2011**.
81. Pan, Y. Z.; Bao, H. Q.; Sahoo, N. G.; Wu, T. F.; Li, L. Water-Soluble Poly(N-isopropylacrylamide)–Graphene Sheets Synthesized via Click Chemistry for Drug Delivery, *Adv. Funct. Mater.* **2011**, *21*, 2754-2763.
82. Fang, M.; Wang, K. G.; Lu, H. B.; Yang, Y. L.; Nutt, S. Covalent polymer functionalization of graphene nanosheets and mechanical, *J. Mater. Chem.*, **2009**, *19*, 7098-7105.
83. Layek, R.; Nandi, A. K. A review on synthesis and properties of polymer functionalized. *Polymer.* **2013**, 54, 5087-5103.
84. Liu, J. Q.; Yang, W. R.; Tao, L.; Li, D.; Boyer, C.; Davis, T. P. Thermosensitive Graphene Nanocomposites Formed Using PyreneTerminal Polymers Made by RAFT Polymerization. *Journal of Polymer Science: Part A: Polymer Chemistry*. **2010**, *48*, 425–433.
85. Kundu, A.; Layek, R. K.; Nandi, A. K. Enhanced fluorescent intensity of graphene oxide–methyl cellulose hybrid in acidic medium: Sensing of nitro-aromatics, *J. Mater. Chem.* **2012**, *22*, 8139.
86. Abell, L.; Adams, P. N.; Monkman, A. P. *Polymer* **1996**, *31*, 5921-5931.
87. Lee, S.; Gleason, K. K. Enhanced Optical Property with Tunable Band Gap of Cross-linked PEDOT Copolymers via Oxidative Chemical Vapor Deposition. *Adv. Funct. Mater.* **2015**, *25*, 85–93.
88. Huang, T. M.; Batra, S.; Hu, J.; Miyoshi, T.; Cakmak, M. Chemical cross-linking of conducting poly(3,4-ethylenedioxythiophene):poly(styrenesulfonate) (PEDOT:PSS) using poly(ethylene oxide) (PEO). *Polymer.* **2013**, *54*, 6455-6462.
89. Pan, L.; Qiu, H.; Dou, C.; Li, Y.; Xu, J.; Shi, Y. Conducting Polymer Nanostructures: Template Synthesis and Applications in Energy Storage. *Int J Mol Sci.* **2010**, *11(7)*, 2636–2657.

90. Kim, H.; Abdala, A. A.; Macosko, C. W. Graphene/Polymer Nanocomposites. *Macromolecules* **2010**, *43*, 6515-6530.
91. Choi, K. S.; Liu, F.; Choi, J. S.; Seo, T. S. Fabrication of Free-Standing Multilayered Graphene and Poly(3,4-ethylenedioxythiophene) Composite Films with Enhanced Conductive and Mechanical Properties. *Langmuir.* **2010**, *26*, 12902-12908.
92. Skotheim, T. A.; Reynolds, J. R. *Handbook of Conducting* Polymers, *3rd ed. Conjugated Polymers: Theory, Synthesis, Properties and Characterization.* CRC Press, **2007**.
93. Casas-Solvas, J. M.; Howgego, J. D.; Davis, A. P. Synthesis of substituted pyrenes by indirect methods. *Org. Biomol. Chem.*, **2014**, *12*, 212.
94. Dewar, M. J. S.; Dennington, R. D. II. DEWAR-PI study of electrophilic substitution in selected polycyclic fluoranthene hydrocarbons. *J. Am. Chem. Soc.*, **1989**, *111*, 3804-3808.
95. Feng, X.; Hu, J. Y.; Redshaw, C.; Yamato, T. Functionalization of pyrene to prepare luminescent materials – typical examples of synthetic methodology. *Chem. Eur. J.* **2016**, *22*, 1-20.
96. Figueira-Duarte, T. M.; Mullen, K. Pyrene-Based Materials for Organic Electronics. *Chem. Rev.* **2011**, *111*, 7260-7314.
97. Rios, P.; Carter, T. S.; Mooibroek, T. J.; Crump, M. P.; Lisbjerg, M.; Pittelkow, M.; Superkar, N. T.; Boons, G. J.; Davis, A. P. Synthetic Receptors for the High-Affinity Recognition of O-GlcNAc Derivatives. *Angew. Chem.* **2016**, *128*, 3448-3453.
98. Hoye, T.; Eklov, B.; Voloshin, M. No-D NMR Spectroscopy as a Convenient Method for Titering, Org. Lett. **2004**, *6*, 2567–2570.
99. Ravat, P.; Lto, Y.; Gorelik, E.; Enkelmann, V.; Baumgarten, M. Tetramethoxypyrene-Based Biradical Donors with Tunable Physical and Magnetic Properties. *Org. Lett.* **2013**, *15 (17)*, 4280–4283.
100. ..... Turbiez, M.; Roncali, J. Oligothienylenevinylenes incorporating 3,4-ethylenedioxythiophene (EDOT) units. *Tetrahedron*. **2005**, *61*, 3045-3053.
101. ..... Turbiez, M.; Frere, P.; Blanchard, P.; Roncali, J. Mixed p-conjugated oligomers of

thiophene and 3,4-ethylenedioxythiophene (EDOT). *Tetrahedron Letters*. **2000**, *41*, 5523.

102. ..... Irvin, J. low oxidation potential electroactive polymers. Ph.D. dissertation, **1998**, University of Florida.

103. ..... Resistivity measurements using the model 2450 SourceMeter SMU instrument and a four-point collinear probe. KEITHLEY, Application Note Series, Number 3247.

104. ..... Yang, H.; Morris, J. J.; Lopina, S. T. Polyethylene glycol–polyamidoamine dendritic micelle as solubility enhancer and the effect of the length of polyethylene glycol arms on the solubility of pyrene in water. *J. Colloid & Interface Sci.* **2004**, *273*, 148–154.

105. ..... Hohnholz, D.; MacDiarmid, A. G.; Sarno, D. M.; Jones, W. E., Jr. Uniform thin films of poly-3,4-ethylenedioxythiophene (PEDOT) prepared by *in-situ* deposition. *Chem. Commun.*, **2001**, 2444-2445.